Kilometric Type III observations : WIND, Ulysses & Stereo

Milan Maksimovic, LESIA

work done by Xavier Bonnin, Vratislav Krupar & Sonja Vidojevic

- **Introduction**
- **Radio Beam Characteristics**
- **Langmuir waves distributions**
- **Open questions and perspectives**

Glasgow-Meudon workshop on "Acceleration and transport of energetic particles: X-ray and radio signatures", Meudon 18-20 May 2010

Observations

- Premières observations [Wild,1950].

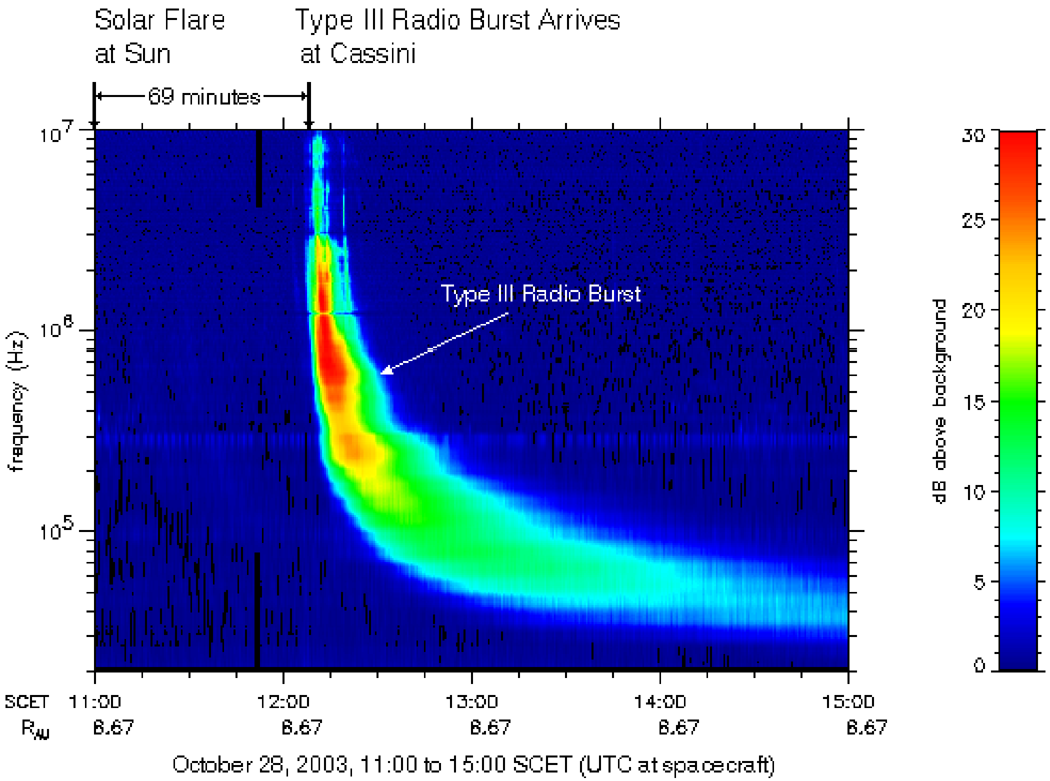

Sursauts radio brefs (sec $\rightarrow$ hrs) et intenses ($\rightarrow 10^{-14}$ W.m^{-2}.Hz^{-1} T $\rightarrow 10^{10}$-10^{17} K) décroissant rapidement depuis les hautes jusqu'aux basses fréquences (GHz $\rightarrow$ kHz).

Le plus souvent associés à des éruptions solaires.

Parfois observés par paire dites *fondamentale* et *harmonique*.
(Faible polarisation)

$\Rightarrow$ Propagation d'une Perturbation. (Faisceau d'électron suprathermals.)

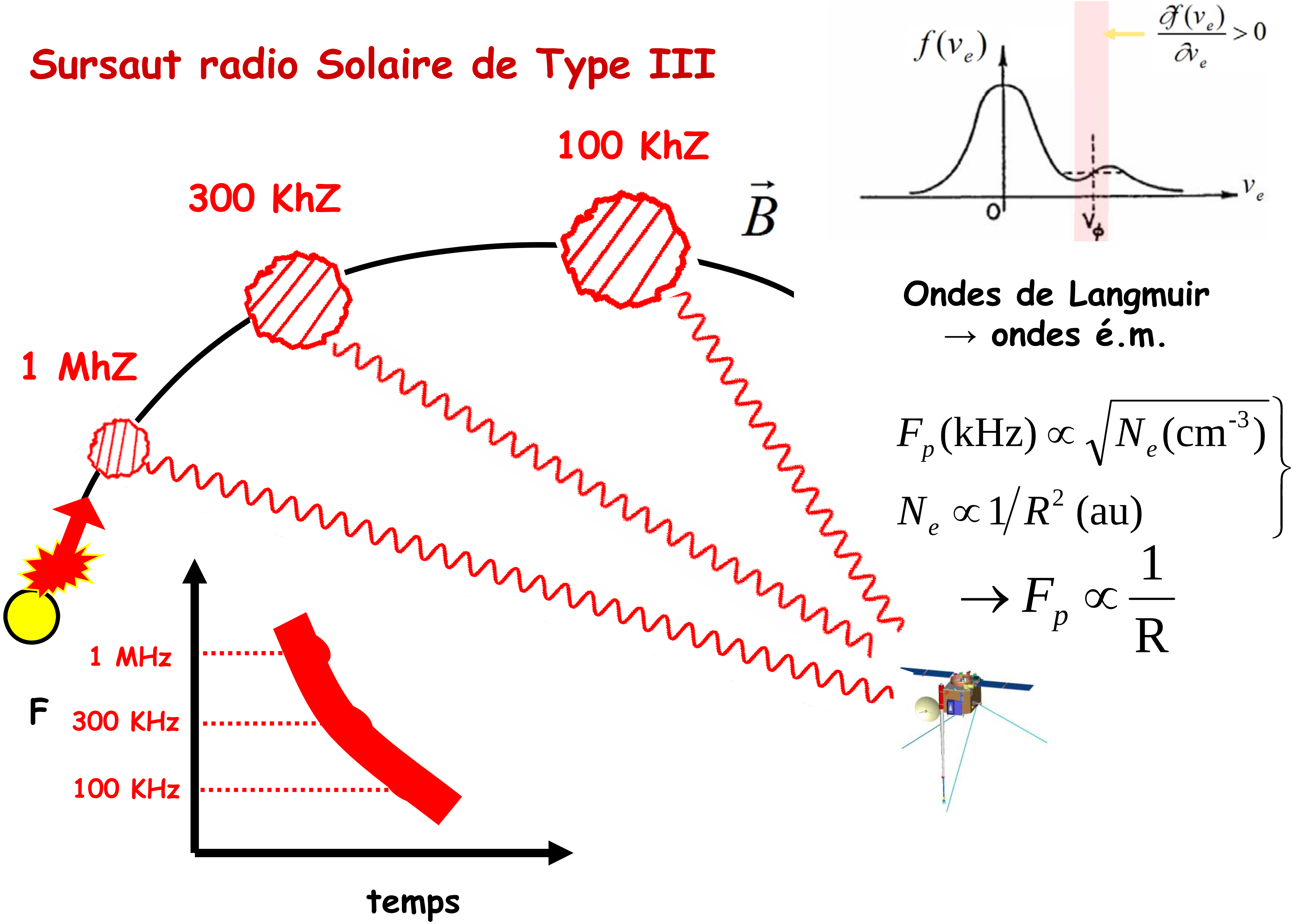

Sursaut radio Solaire de Type III
100 KhZ
300 KhZ
1 MhZ
$\vec{B}$
$f(v_e)$
$\frac{\partial f(v_e)}{\partial v_e} > 0$
v_e
0
V_ϕ
Ondes de Langmuir
→ ondes é.m.
$F_p(\text{kHz}) \propto \sqrt{N_e(\text{cm}^{-3})}$
$N_e \propto 1/R^2\ (\text{au})$
$\rightarrow F_p \propto \frac{1}{R}$
F
1 MHz
300 KHz
100 KHz
temps

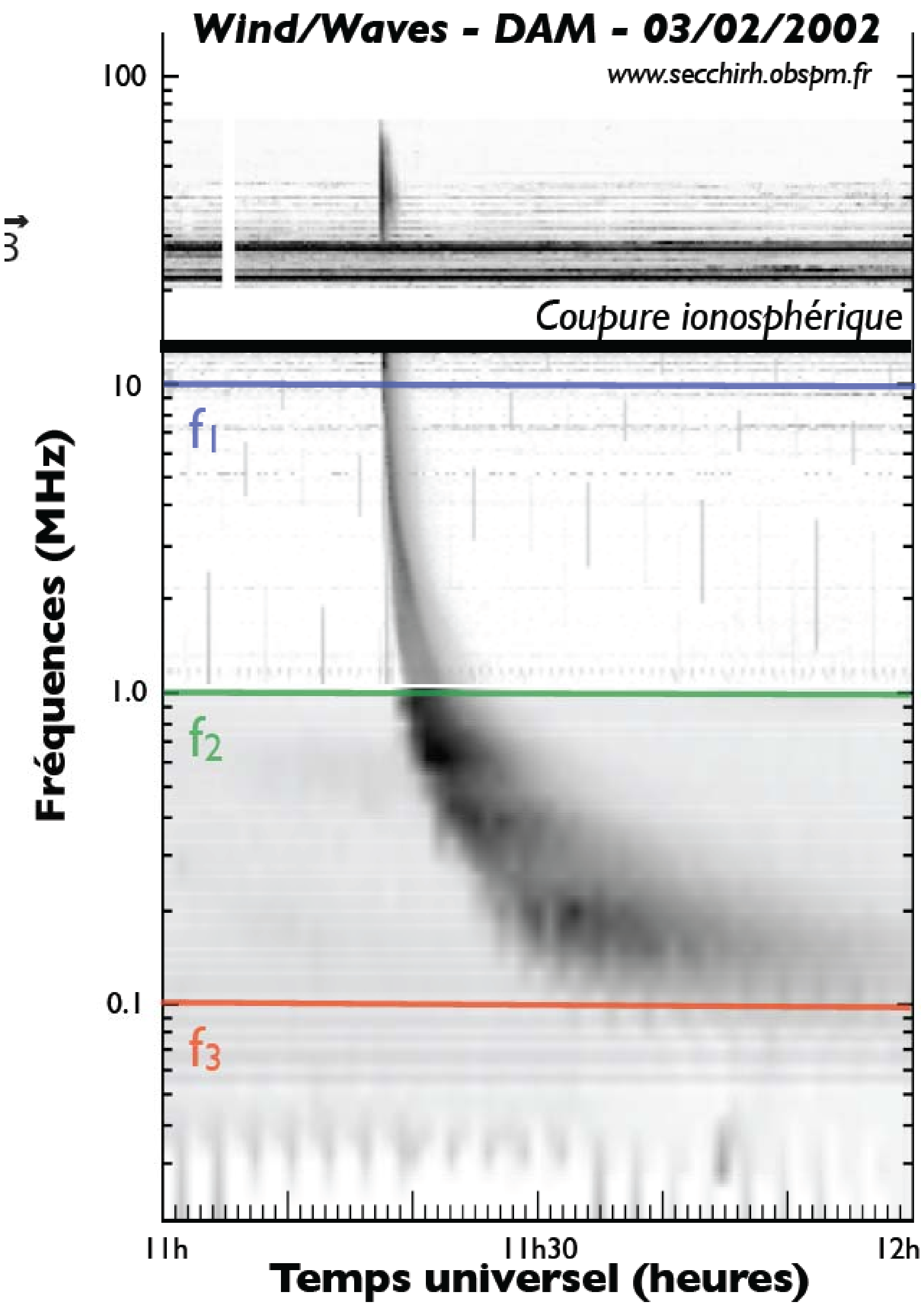
Wind/Waves - DAM - 03/02/2002
www.secchirh.obspm.fr
100
Coupure ionosphérique
10
f_1
1.0
f_2
0.1
f_3
Fréquences (MHz)
11h
11h30
12h
Temps universel (heures)

Observations

- Profil temporel

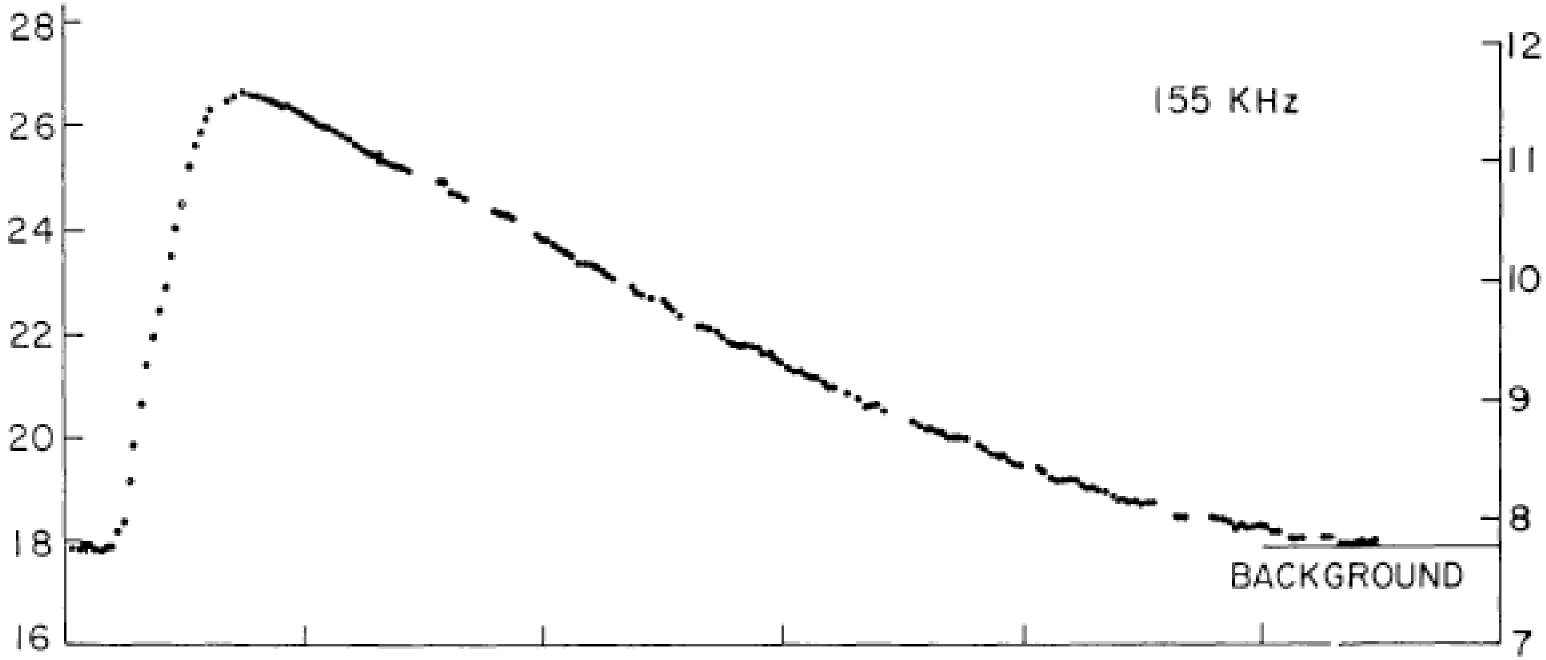

- Temps de montée << Temps de descente (exponentiel)
- Pour $4x10^5\ s^{-1} < f\ (Hz)/2\pi < 1.8x10^7\ s^{-1}$:

$I_{dec} \propto \exp[-t/td]$ [Evans et al. ,1973]

$(1/td = 10^{-9}(f\ (Hz)/2\pi)^{(1.09\pm0.05)})$

Temps de descente td << Dispersion par collision (Coulomb) dans le plasma (>10td).

20 Novembre 2006

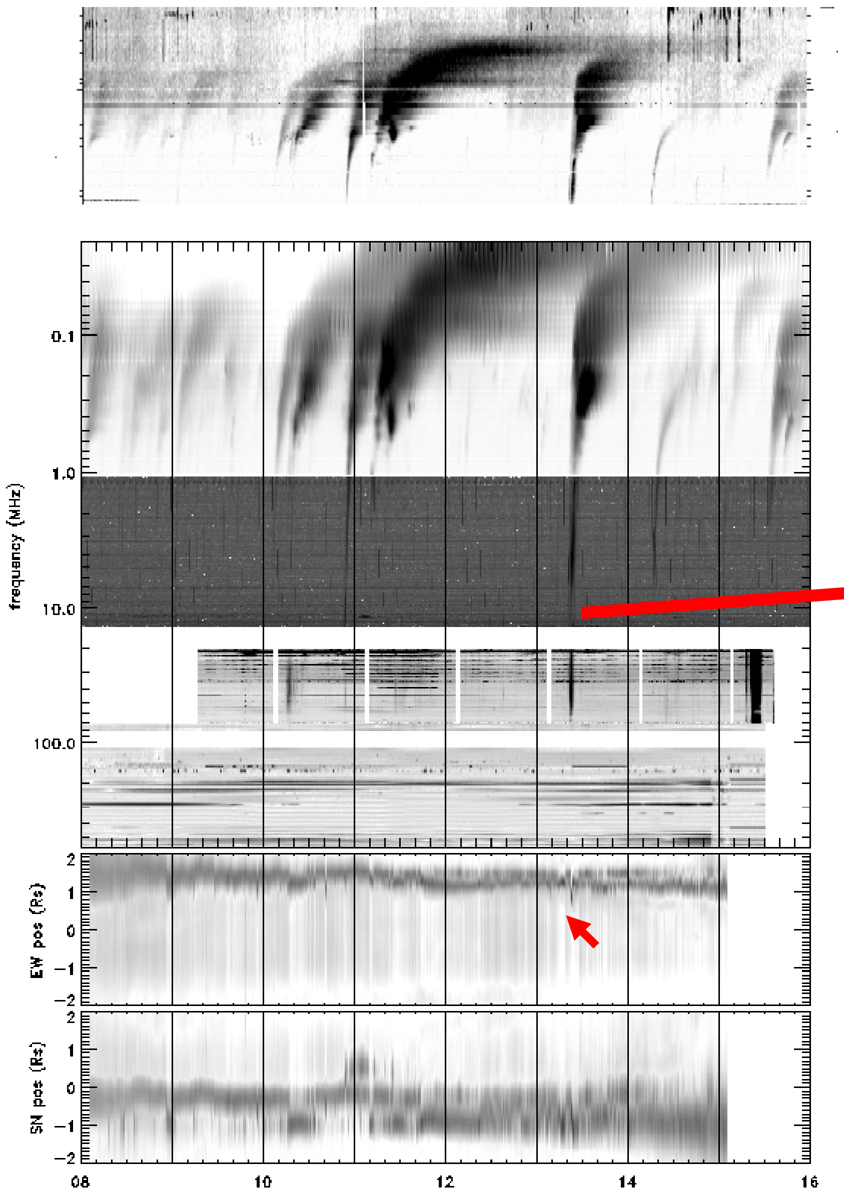

SWAVES (zoom 3H)

WIND/
WAVES

DAM (10-80 MHz)

ARTEMIS (20 to 650)

NRH (10 fréq. 150 et 450 MHz)

- Spectres, zoom
- Films (10sec) NRH
- Temps réel NRH
- CMEs (SOHO SECCHI)

http://secchirh.obspm.fr/

Type II non observés
(minimum d'activité)

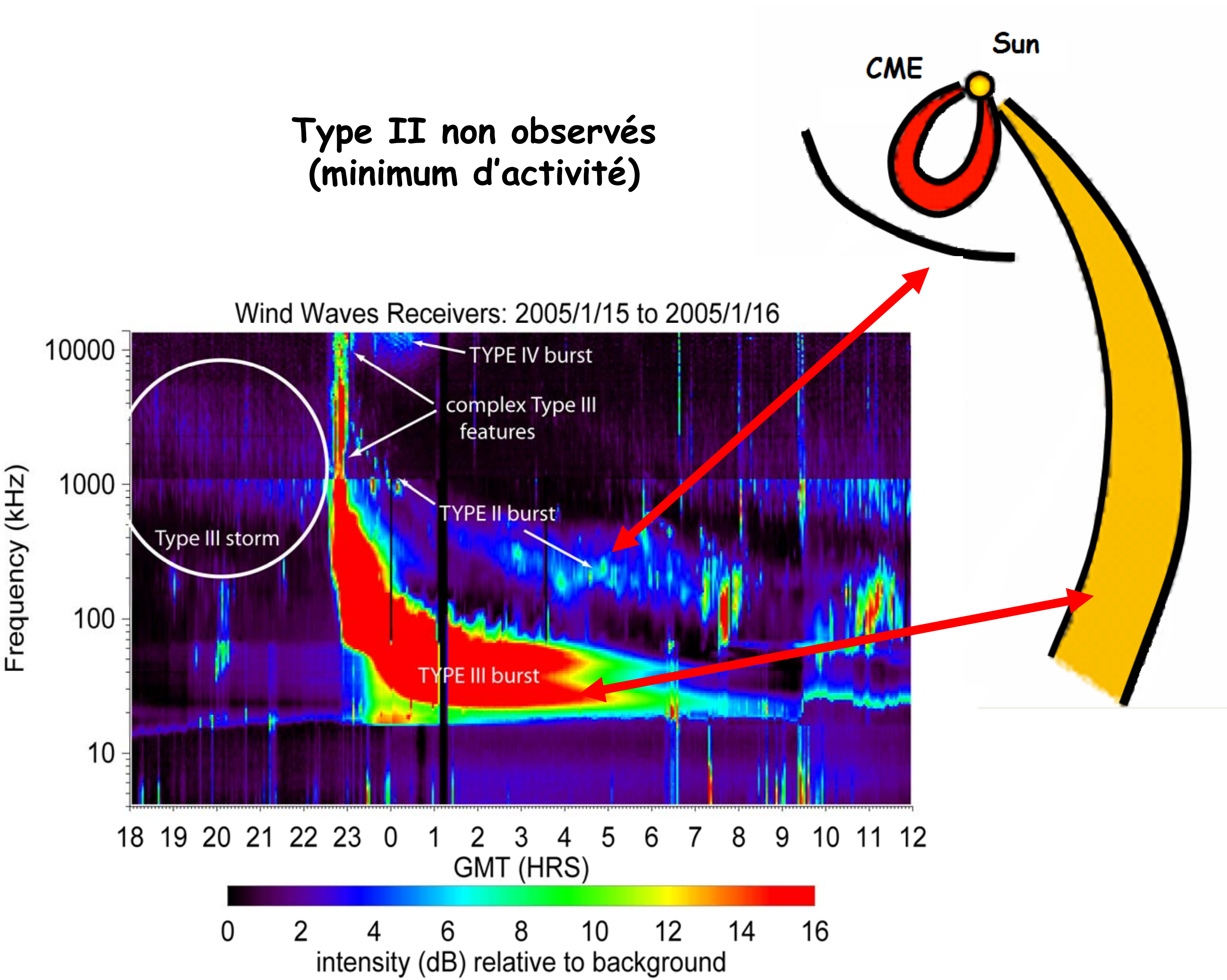

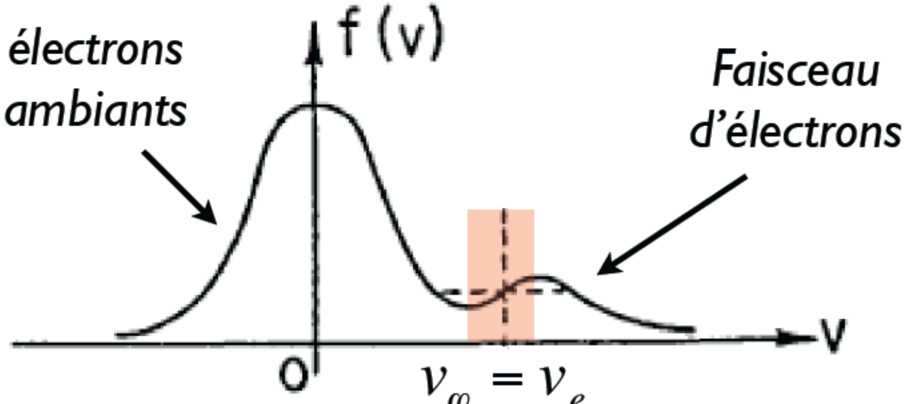

$v_\varphi = v_e$

$$\Gamma_L(s^{-1}) \propto \frac{\partial f(v)}{\partial v}$$

Couplage onde-particule
(Instabilité "bump-on-tail")

Croissance d'ondes électrostatiques de Langmuir
L(fp)

Couplage onde-onde
(Interactions "3-ondes")

$$\begin{cases} L + S \rightarrow F(f_p) \\ L + S \rightarrow L' \\ L + L' \rightarrow H(2f_p) \end{cases}$$

(S = ondes acoustiques ioniques)

$$\Gamma_F(s^{-1}) \mid \Gamma_H(s^{-1})$$

Rayonnement électromagnétique radio :
Fondamental F(f_p)
Harmonique H($2f_p$)

Sturrock (1964) dilema ➔ Necessity of saturation mechanisms

(If no saturation ⇒
$\tau_{growth} \propto 10^7 sec^{-1}$: $d_{faisceau}$ < 1 km ; $Amplitude_{Ltheo}$ >>$Amplitude_{Lobs}$)

Stochastic Growth Theory

Condition de résonance onde-particule (Vavilov-Cerenkov) : $\omega = \vec{k}.\vec{v}_e$

➔ Ondes dans la direction $\vec{k}$ sont émises par des particules dont la vitesse projetée dans cette direction $v_{\vec{k}} = v_e \cos\theta$ est égale à la vitesse de phase de l'onde ; soit

$$v_{\vec{k}} = v_{ph} \quad (\text{avec } v_{ph} = c/n_j)$$

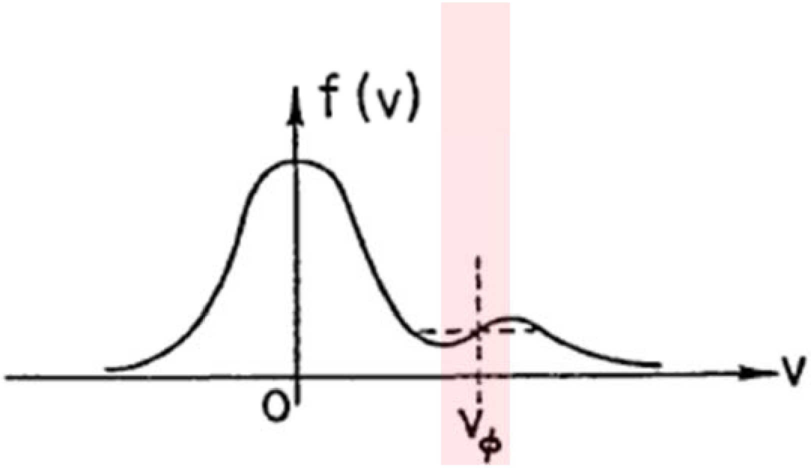

Density fluctuations cause Vϕ fluctuations

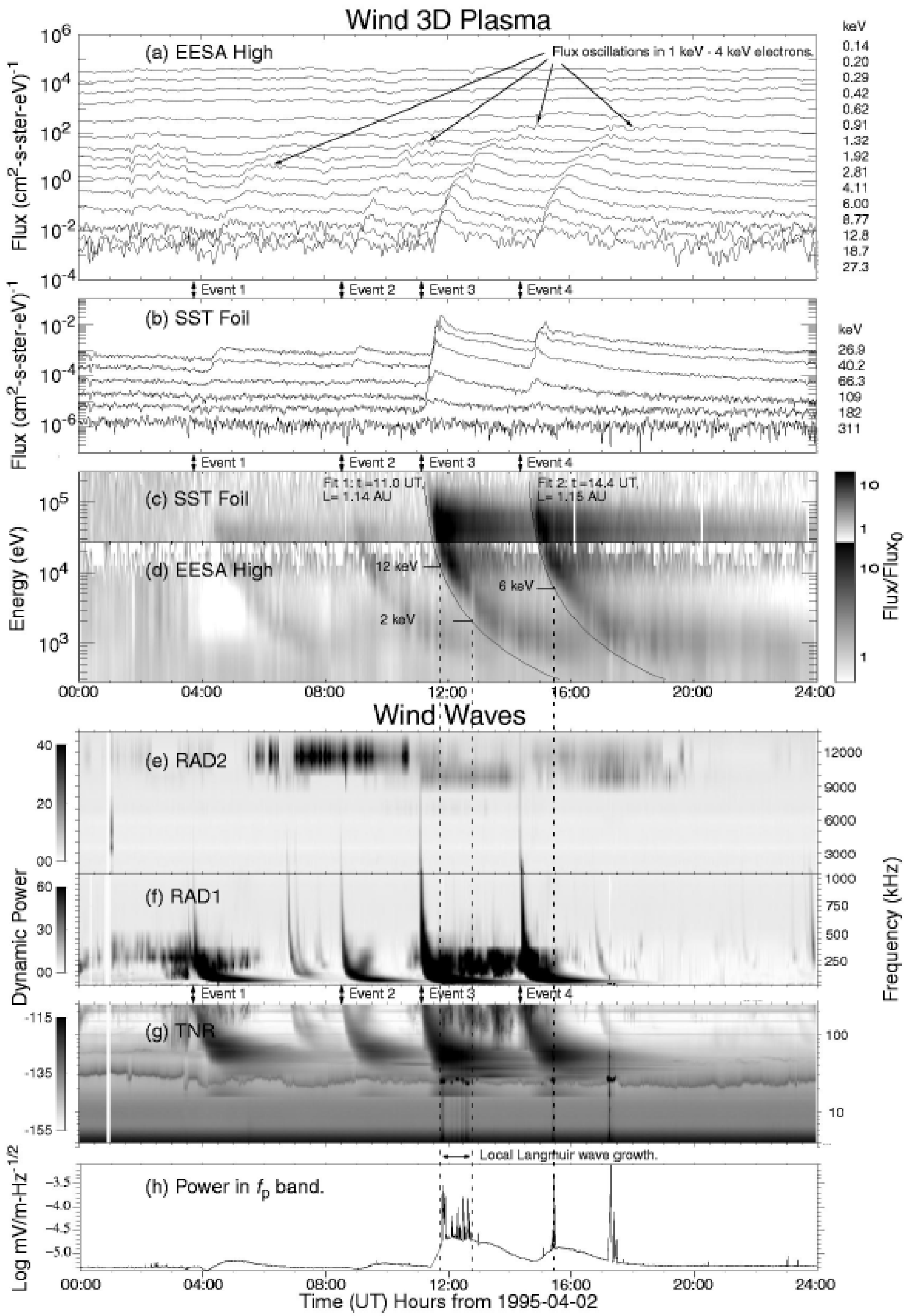

Ergun et al., 1998

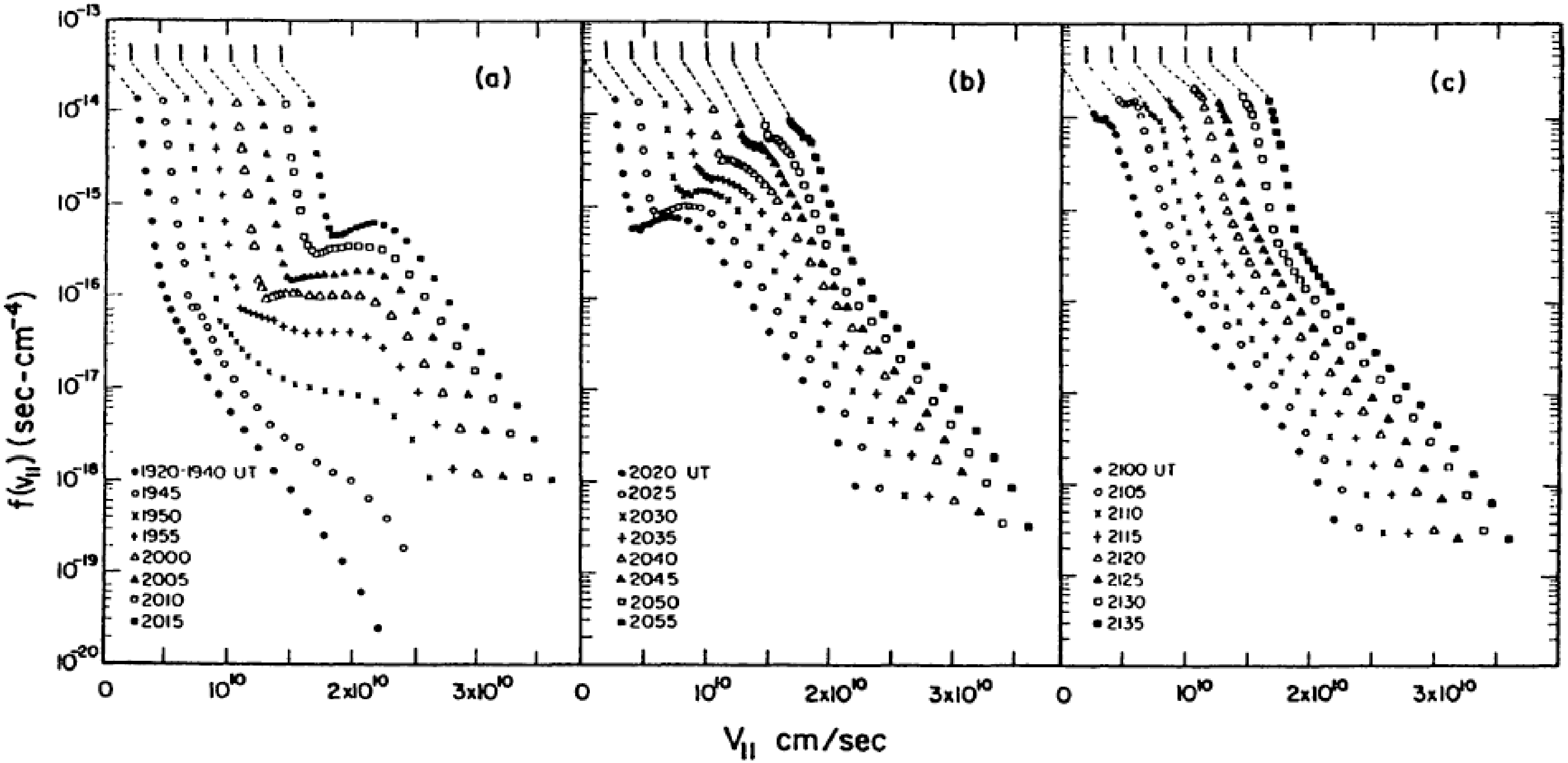

[Lin et al. 1981]

$$\partial f(v_{//})/\partial v_{//} \approx 10^{-15} - 10^{-14} \quad (m^{-5}s^{2})$$

Type III radio emission diagram observed by Wind and Ulysses

Xavier Bonnin

STEREO/WAVES Daily Summary - 22-Feb-2010 (DOY 053)

Ahead source file = swaves_ahead_2010_053_1_04.fin
Ahead PSE Angle = xxx.x

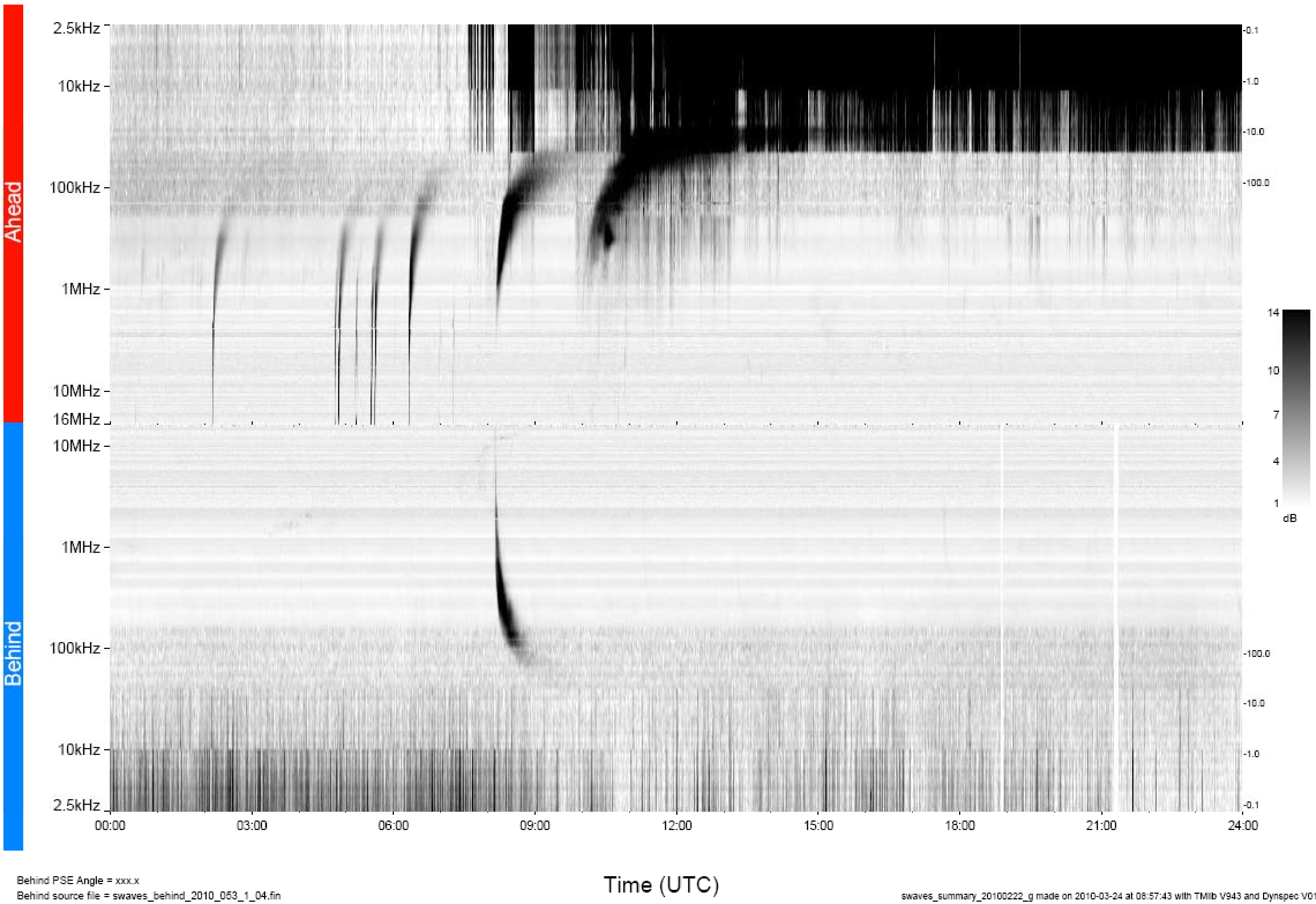

Behind PSE Angle = xxx.x
Behind source file = swaves_behind_2010_053_1_04.fin

swaves_summary_20100222_g made on 2010-03-24 at 08:57:43 with TMlib V943 and Dynspec V015

Localisation et Mesure du diagramme de rayonnement (T de brillance)

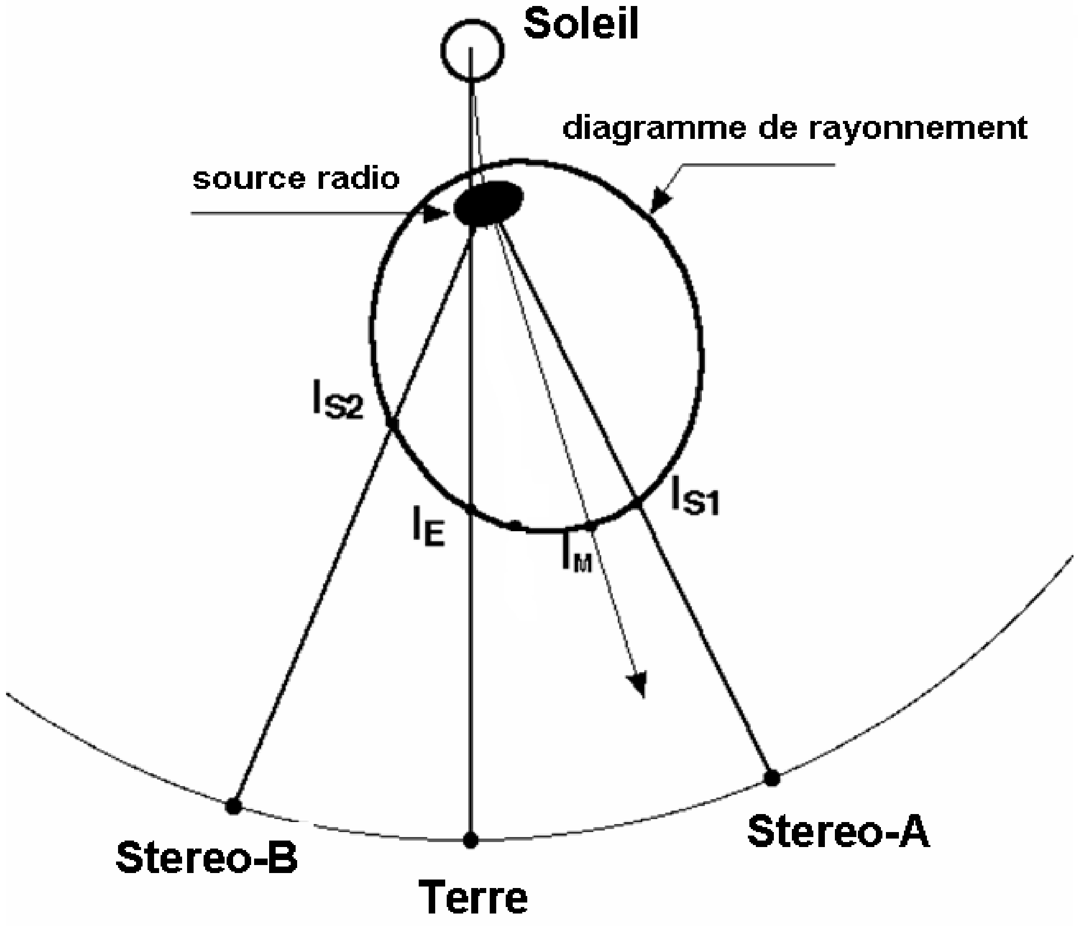

Mesure stéréoscopique du diagramme

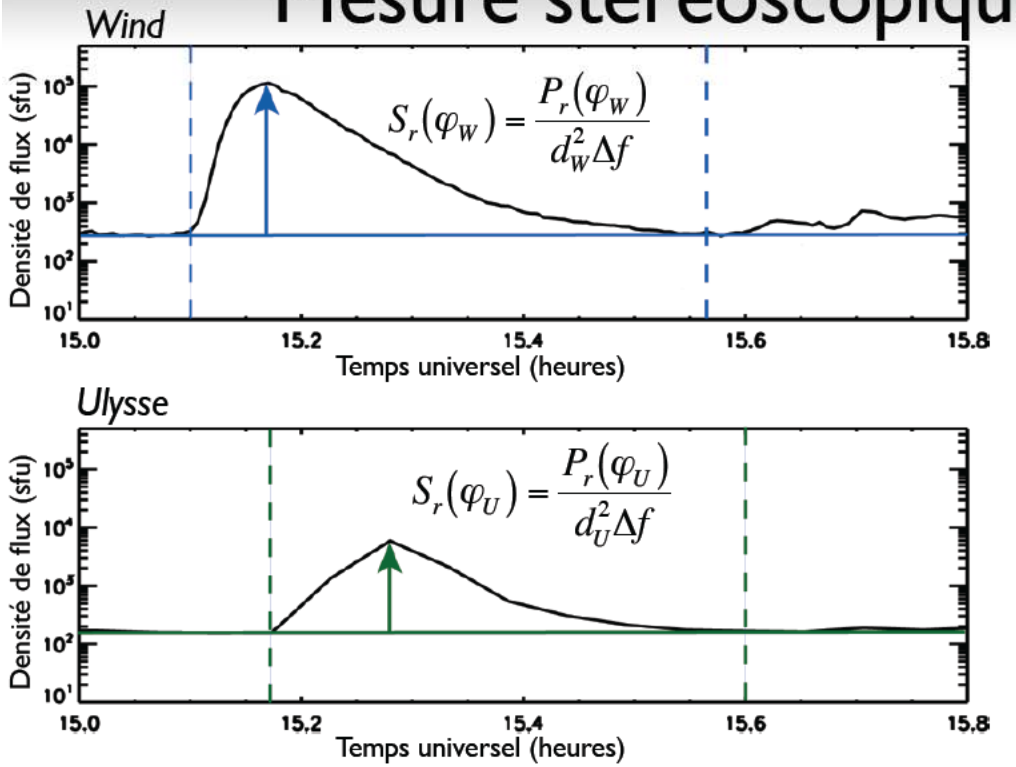

➡N sursauts

➡2 observateurs

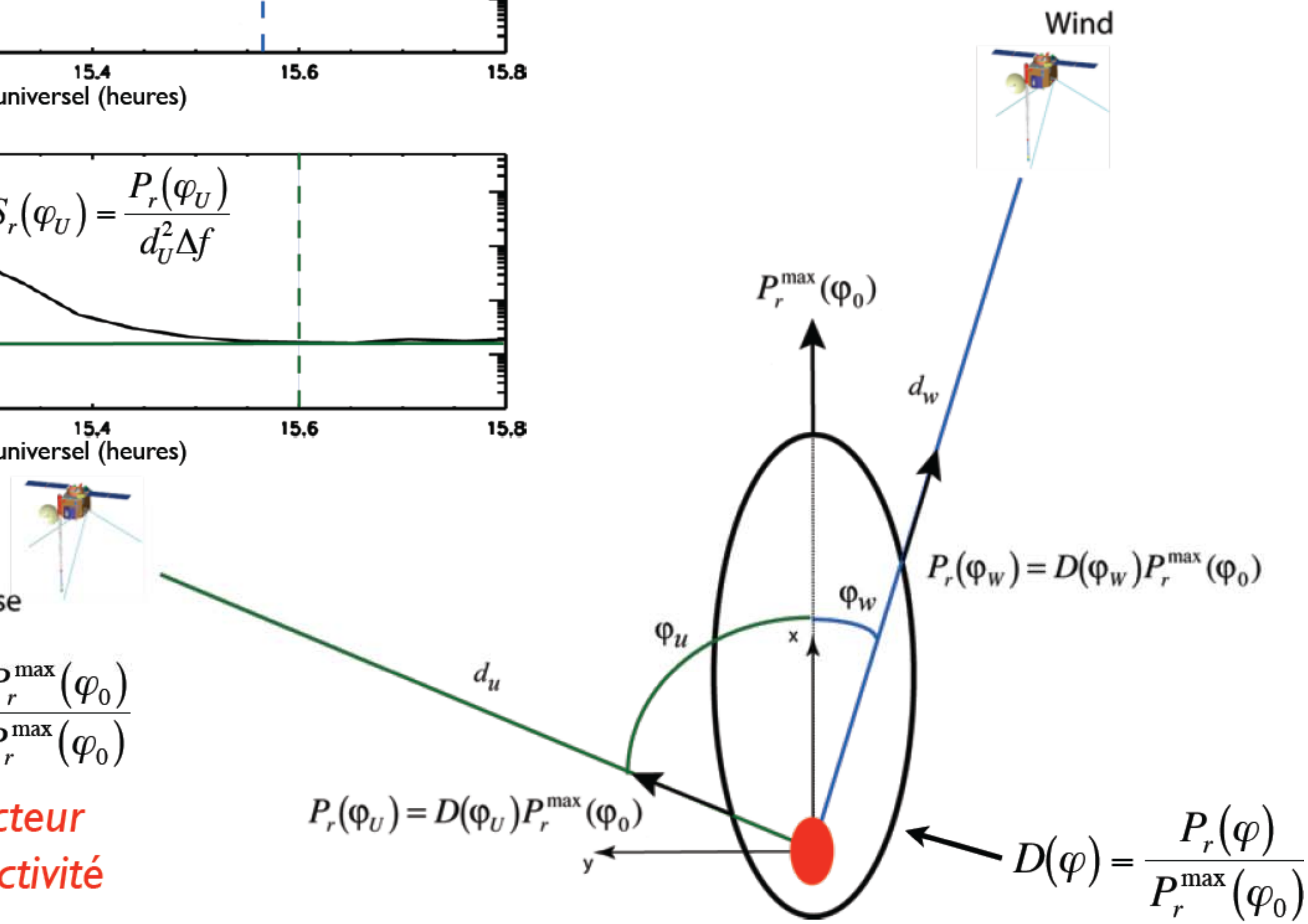

$$R = \frac{P_r(\varphi_W)}{P_r(\varphi_U)} = \frac{D(\varphi_W) P_r^{max}(\varphi_0)}{D(\varphi_U) P_r^{max}(\varphi_0)}$$

$$R = \frac{D(\varphi_W)}{D(\varphi_U)}$$

R : *Facteur de directivité*

Source Localization : density model

Les faisceaux se propagent le long de lignes de champ magnétique ouvertes :

Trajectoire spirale → $r_s - r_{AR} = -\frac{V_{sw}}{\omega_{\Theta}}\left(l_s - l_{AR}\right)\ ;\ \lambda_s = \lambda_{AR}$

Modèle de densité en 1/r²

$$r_s(ua) \approx \frac{9\sqrt{N_e^{1ua}}}{f(kHz)}$$

Identification des régions actives
(corrélations avec sursauts X/Ha, RHN)

$$(l_{AR}, \lambda_{AR}, r_{AR} \approx 1R_{\Theta})$$

$$\varepsilon_{(l_{AR},\lambda_{AR})} = \pm 25^{\circ}$$

Mesures *in situ*
(Wind/SWE à tw)

$$\left(N_e^{1ua}, V_{sw}\right)$$

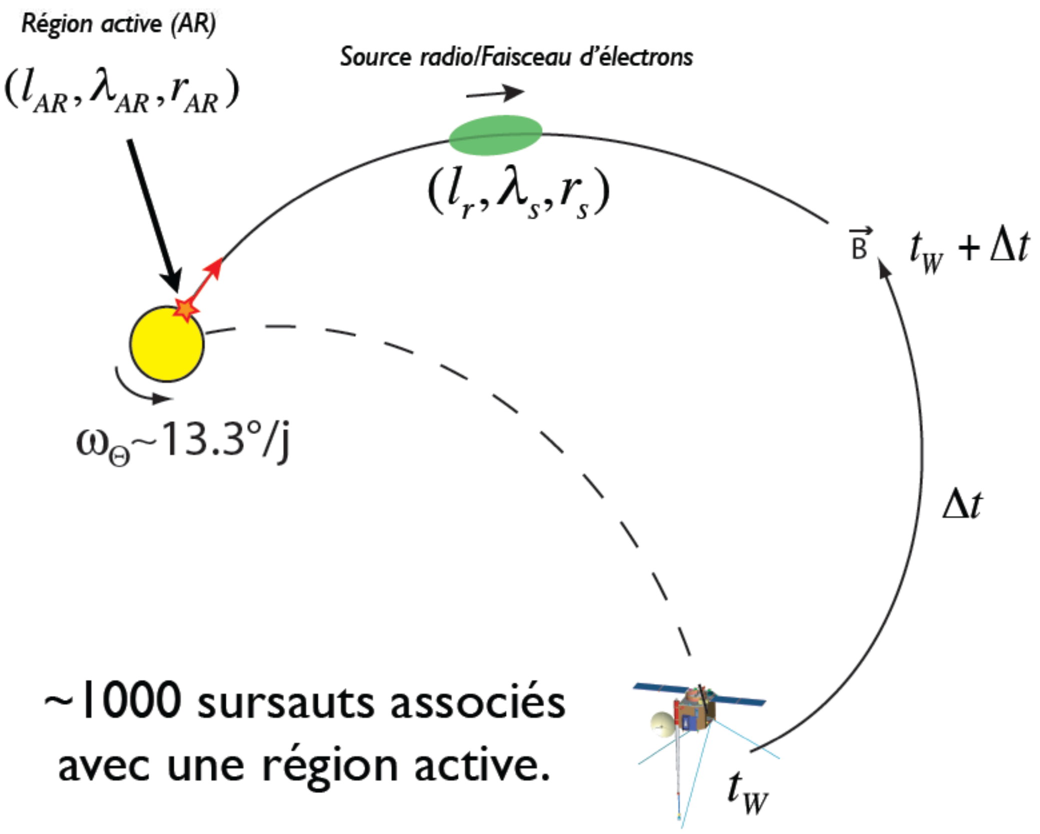

~1000 sursauts associés avec une région active.

Identification des régions actives $\longrightarrow (l_s, \lambda_s) \longrightarrow$ ~1000 sursauts

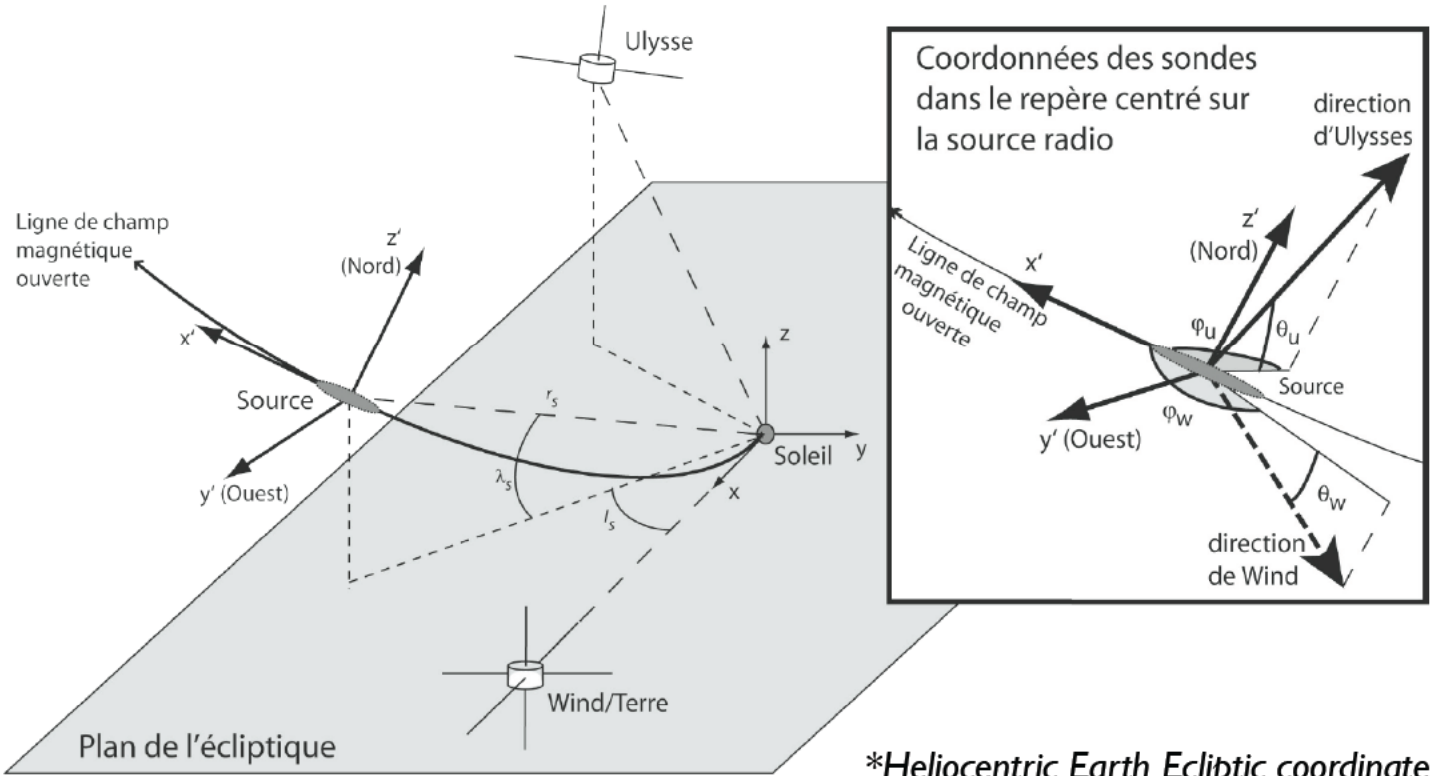

**Heliocentric Earth Ecliptic coordinate system*

Source Localization : Direction Finding

Sur un satellite qui spinne (WIND)
→ La modulation du signal donne
- θ , φ
- taille de la source
- paramètres de polarisation S, Q, U V

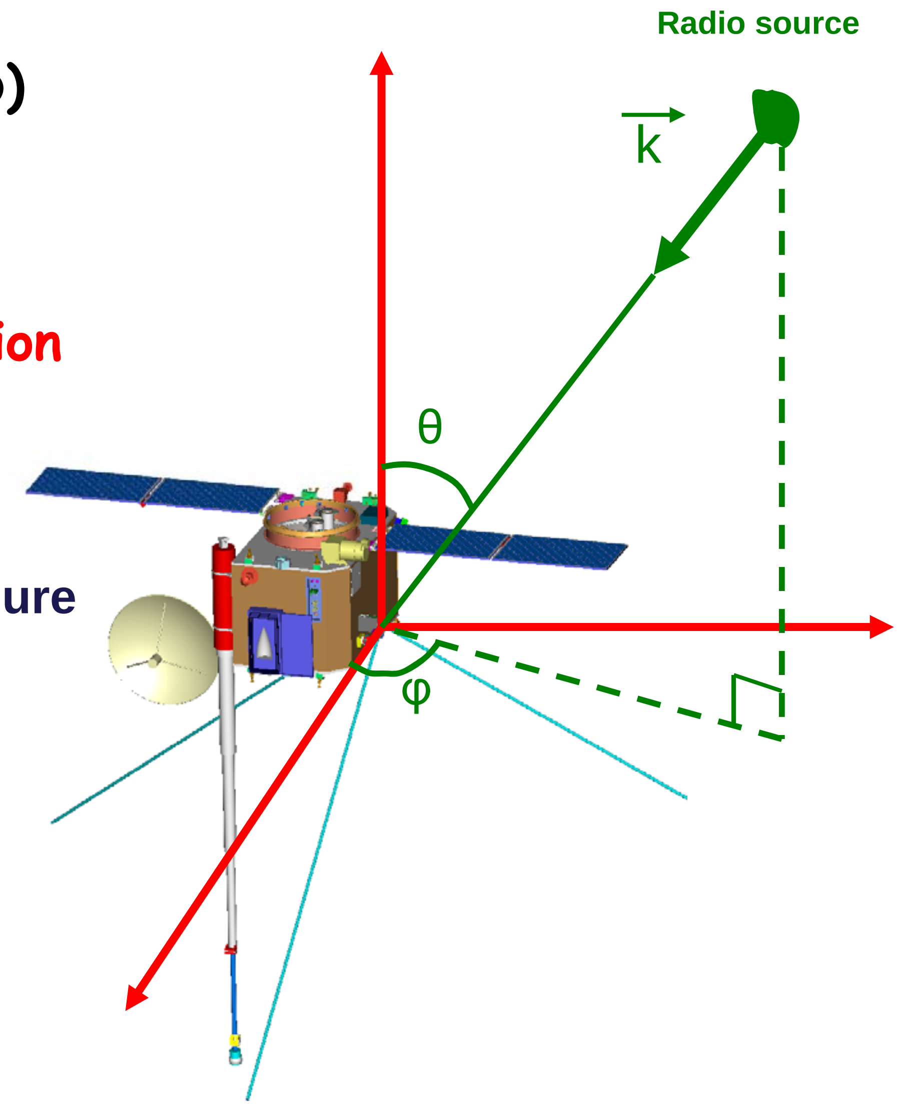

Sur un satellite stabilisé 3-axes on mesure directement

- Auto-correlations (Ex, Ey & Ex)
- Cross-correlations

→ Pas encore appliqué pour des sources radio solaires

Presentation by V. Krupar

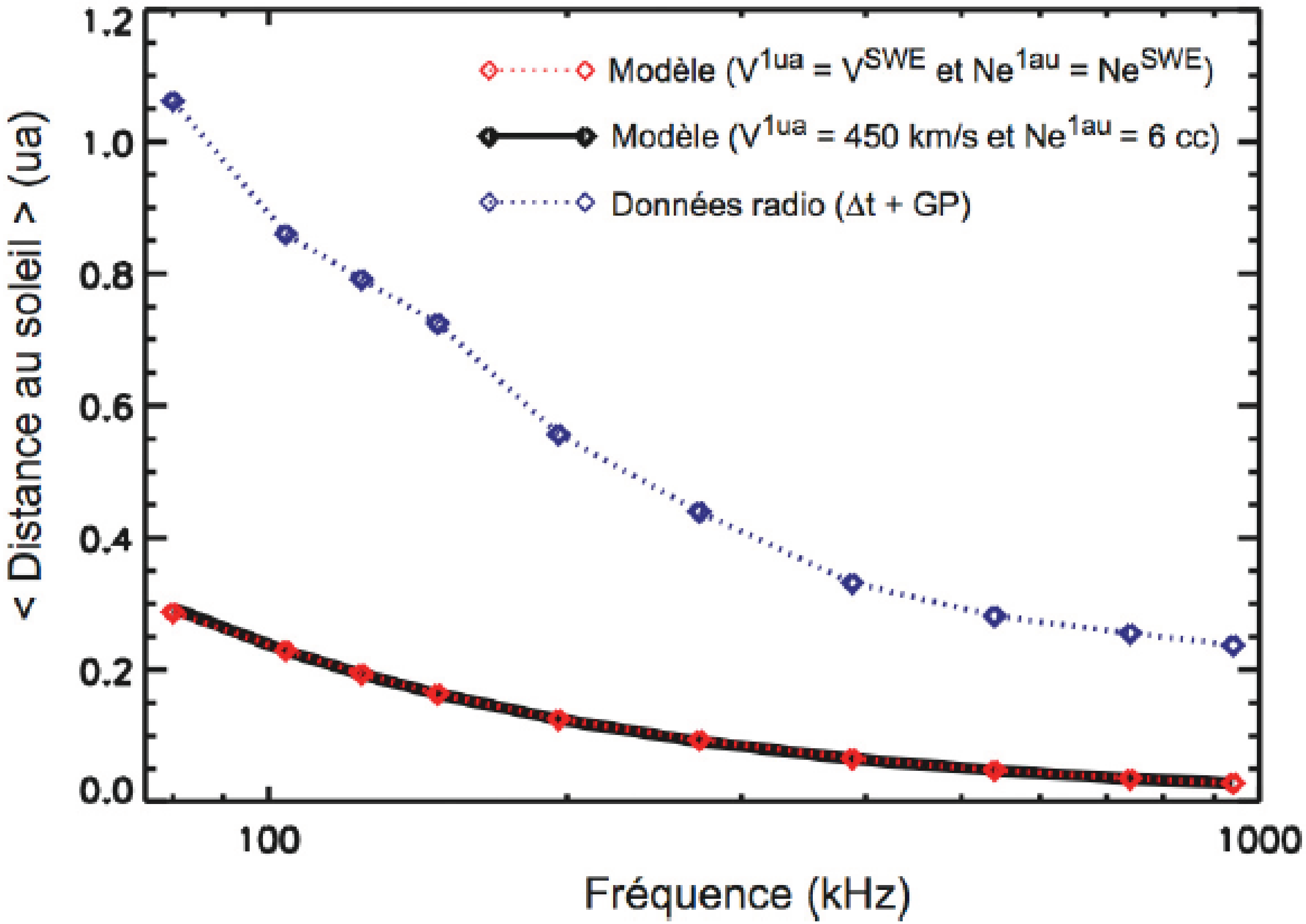

Modèle (V^1ua = V^SWE et Ne^1au = Ne^SWE)
Modèle (V^1ua = 450 km/s et Ne^1au = 6 cc)
Données radio (Δt + GP)
< Distance au soleil > (ua)
1.2
1.0
0.8
0.6
0.4
0.2
0.0
100
1000
Fréquence (kHz)

~ 2000 events

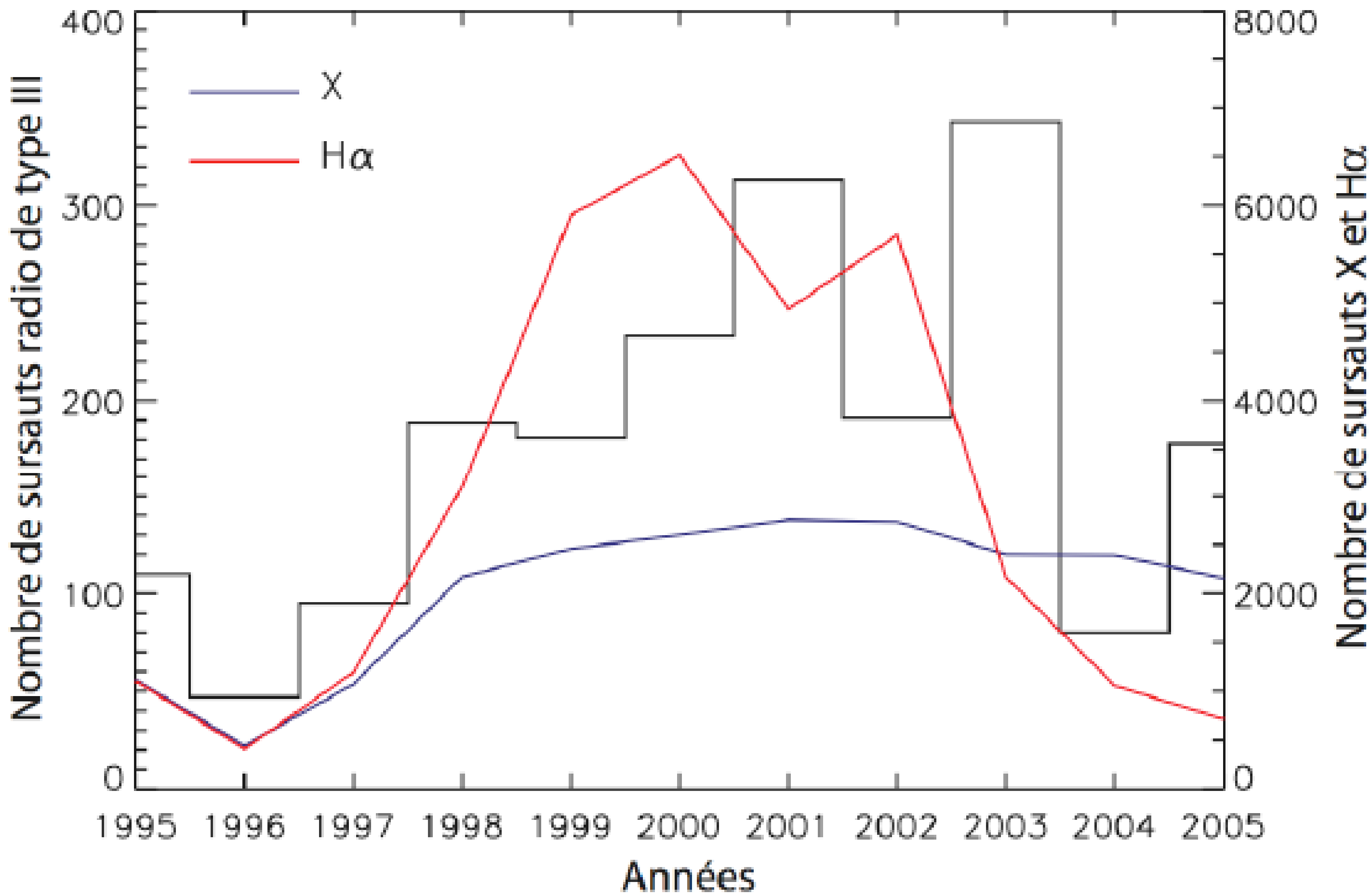

FIGURE 2.5 – *Nombre annuel de sursauts radio de type III (échantillon d'environs deux mille sursauts observés par la sonde Wind entre 1995 et 2005) (trait plein noir), X et H_α (données fournies par le NDGC) (trait plein bleu et rouge) en fonction du temps. Les trois courbes suivent globalement la même évolution au cours du cycle solaire 23 qui couvre cette période ; le minimum solaire se situe en 1996, le maximum vers 2001.*

Diagramme en fonction de la longitude

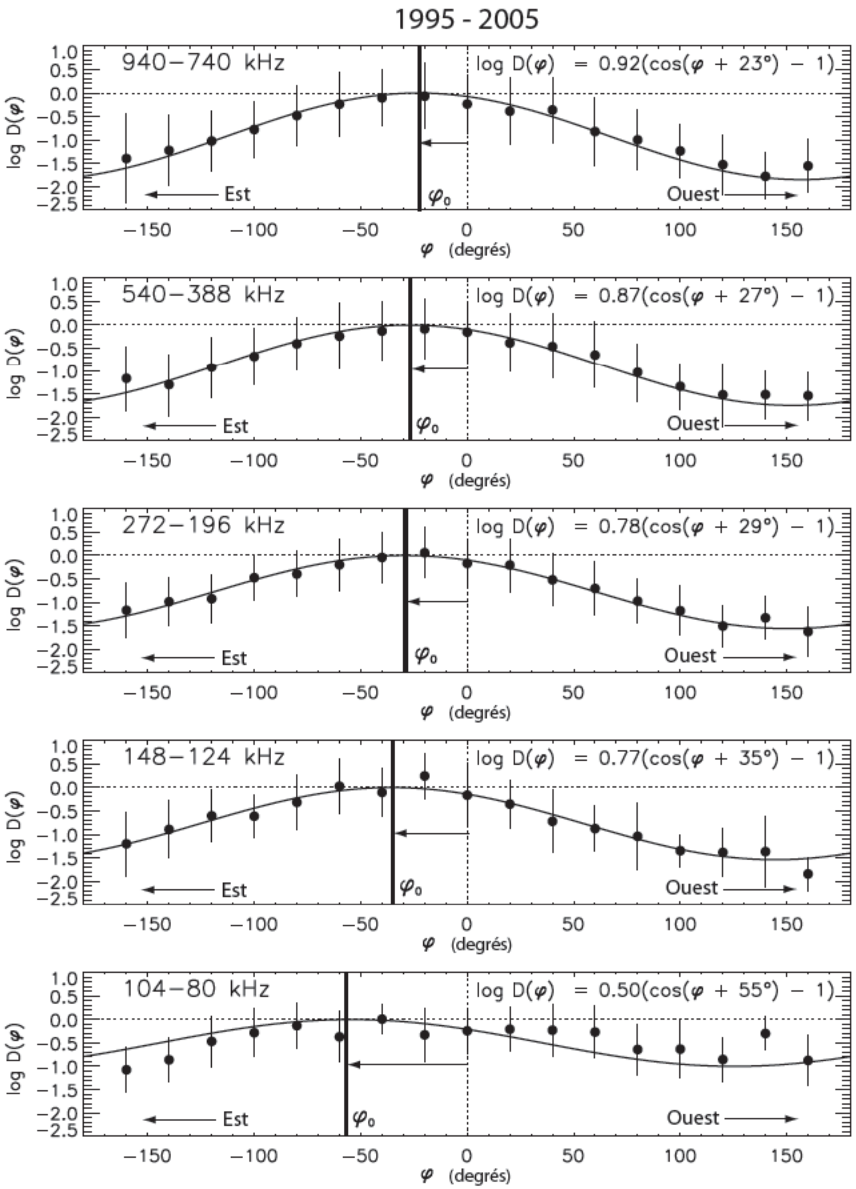

- Ouverture angulaire $\Delta\varphi_2$ du diagramme large :
  - 100° à 1000 kHz
  - 120° à 100 kHz

- Visibilité des sursauts aux grands angles :
  - 100 fois plus faibles à 1000 kHz
  - 10 fois plus faibles à 100 kHz

- Déviation vers l'est de l'axe du diagramme par rapport à la direction du φ_0 champ magnétique local :
  - 23° à 1000 kHz
  - 55° à 1000 kHz

Bonnin et al. 2008

Puissance radio rayonnée

$$P(t,f) = \frac{S(t,f,\varphi)\Delta f d^2}{D(f,\varphi)}\Omega$$

Angle solide : $\Omega = \int\int_{4\pi} D(\theta,\phi) d\Omega.$

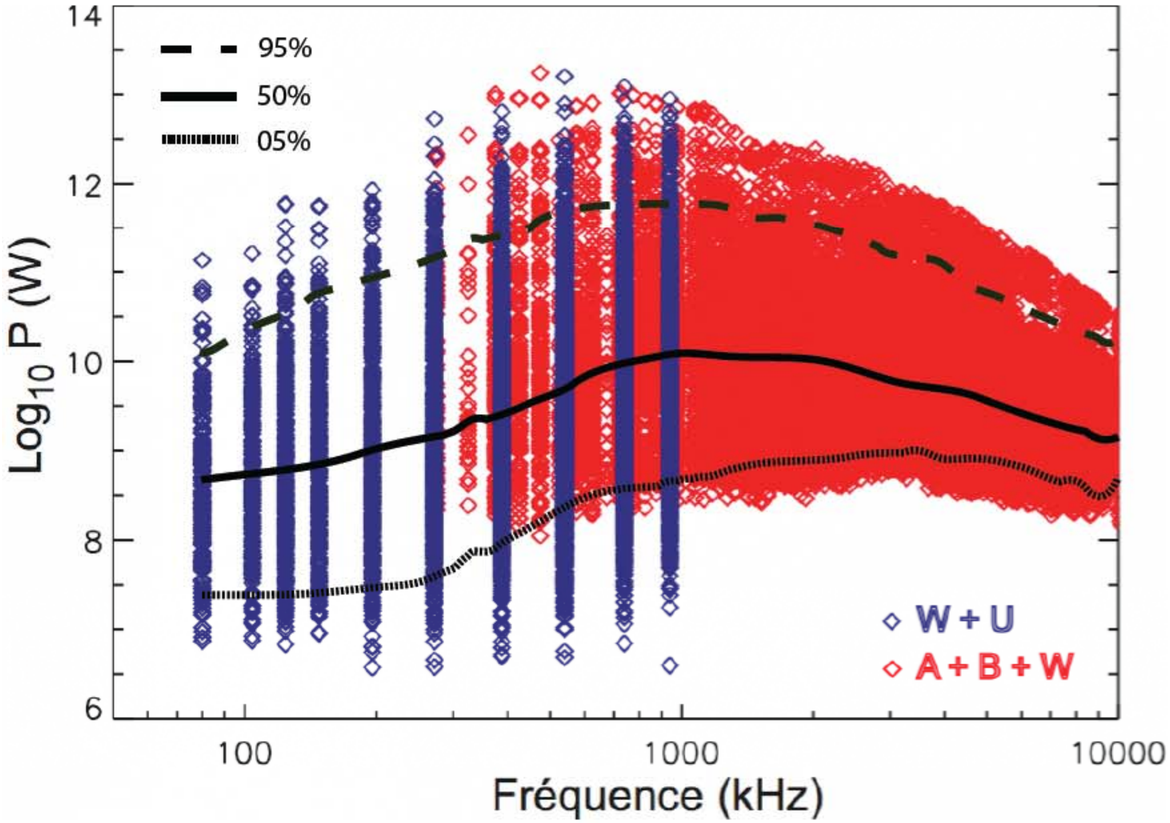

- Distribution de puissance log-normale?
- Maximum autour de ~1 MHz (R ~ 6R☉)
  - Convergence des faisceaux

    (Dulk et al. 2001)
  - Décélération des électrons + directivité

    (Weber 1978)

Correction par rapport à la radiale

$$v = \frac{1}{\cos(\psi)} \frac{dr}{df} \frac{df}{dt}$$

Dérive en fréquence (données radio)

Profil radial de densité

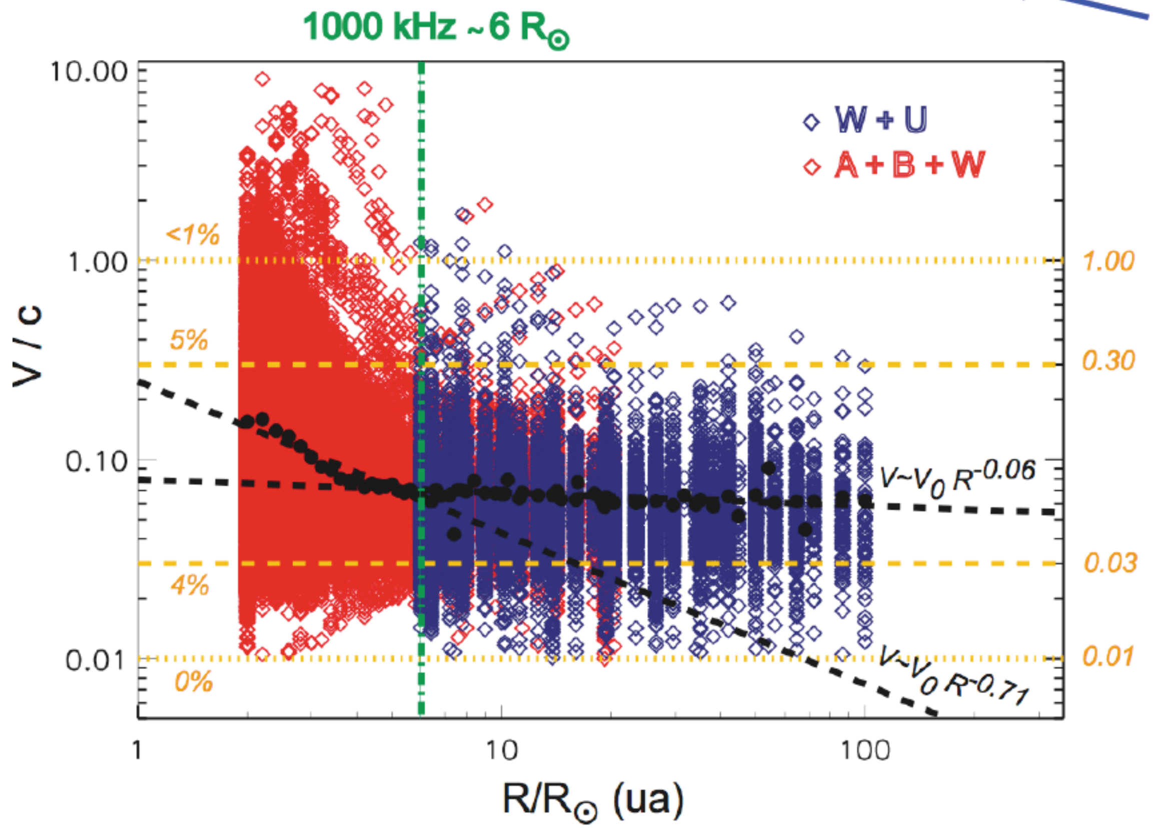

- $R < 6\ R_\odot$
  ➡ Décélération “rapide” des électrons du faisceau.

- $R > 6\ R_\odot$
  ➡ Décélération “lente” des électrons du faisceau.

$V_{initiale}$ et V_{finale} sont décorrélées.

(Poquérusse et al 1996)

Perte d’énergie cinétique du faisceau plus efficace dans la couronne.
Rôle prédominant des propriétés du milieu ambiant sur les mécanismes d’émission

In-situ distribution of Langmuir waves

Sonja Vidojevic

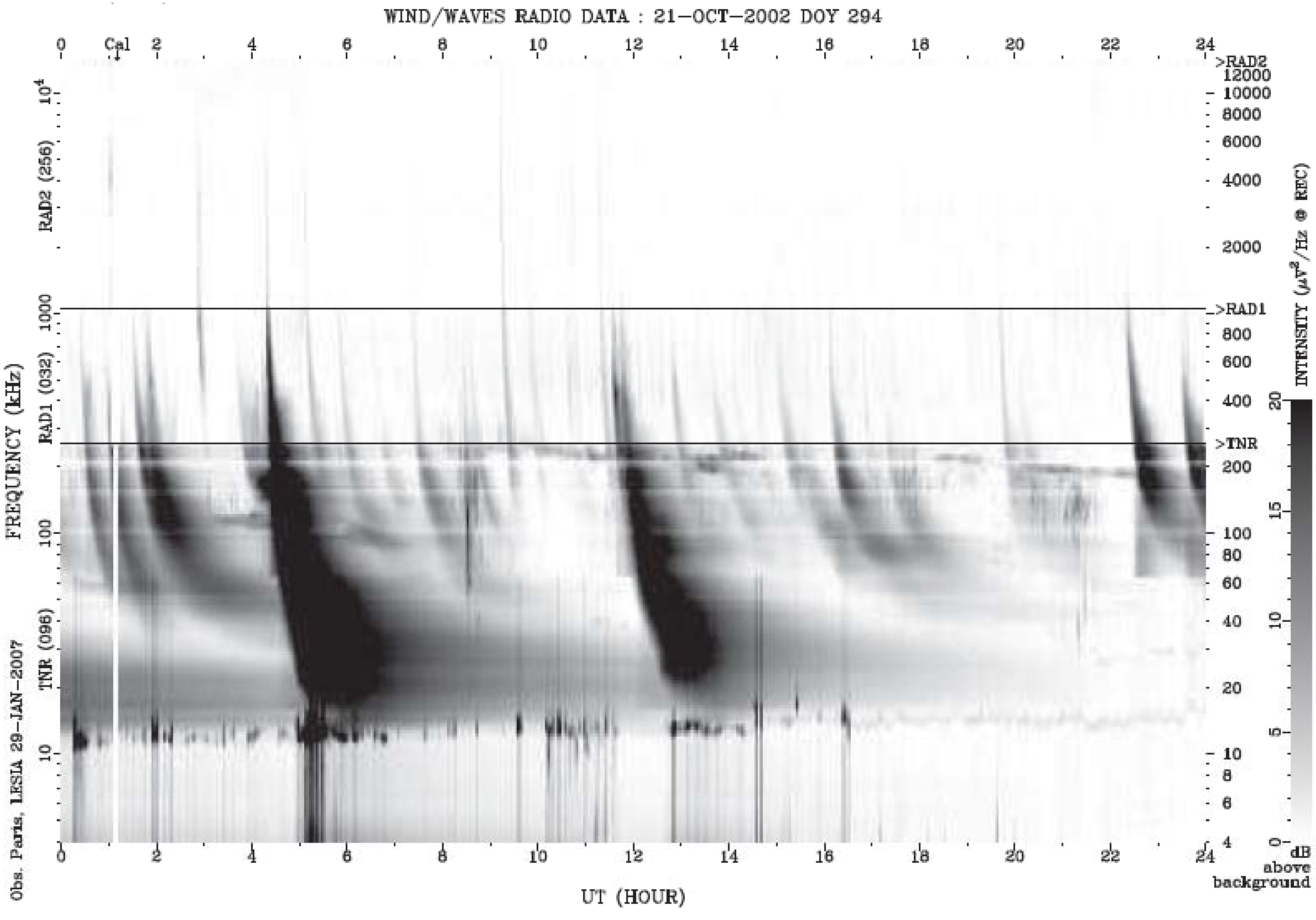

WIND/WAVES RADIO DATA : 21-OCT-2002 DOY 294
Cal
FREQUENCY (kHz)
RAD2 (256)
RAD1 (032)
TNR (096)
>RAD2
>RAD1
>TNR
UT (HOUR)
INTENSITY (μV²/Hz @ REC)
dB above background
Obs. Paris, LESIA 29-JAN-2007

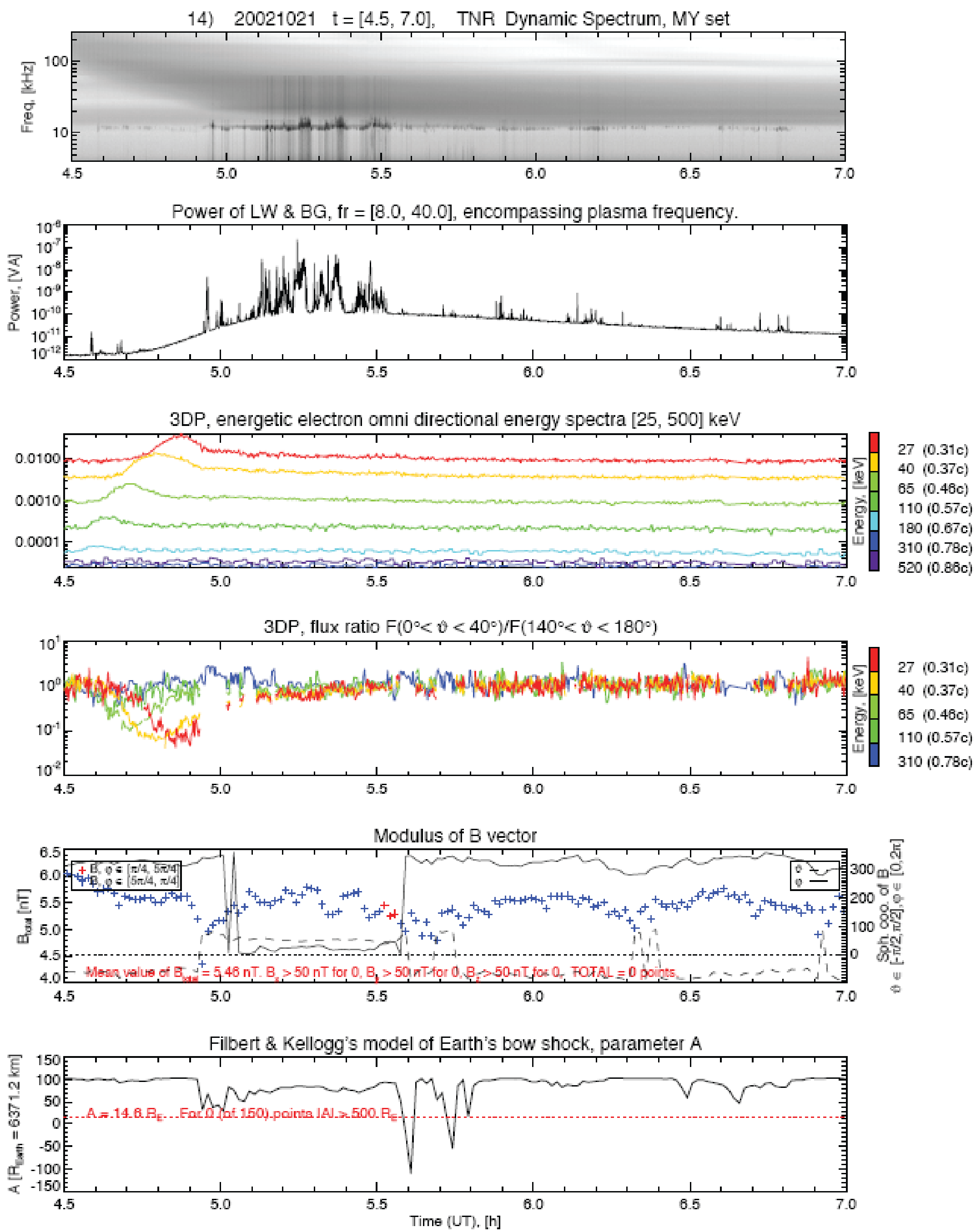

14) 20021021 t = [4.5, 7.0], TNR Dynamic Spectrum, MY set
Freq. [kHz]
Power of LW & BG, fr = [8.0, 40.0], encompassing plasma frequency.
Power, [V/A]
3DP, energetic electron omni directional energy spectra [25, 500] keV
27 (0.31c)
40 (0.37c)
65 (0.46c)
110 (0.57c)
180 (0.67c)
310 (0.78c)
520 (0.86c)
Energy, [keV]
3DP, flux ratio F(0°< ϑ < 40°)/F(140°< ϑ < 180°)
Modulus of B vector
Filbert & Kellogg's model of Earth's bow shock, parameter A
Time (UT), [h]

The stochastic growth theory (SGT) describes situations in which an unstable distribution of particles interacts self-consistently with its driven waves in an inhomogeneous plasma environment and evolves to a state in which the particle distribution fluctuates stochastically about a state close to time and volume averaged marginal stability. These fluctuations drive waves so that the wave gain, $G = 2\ln(E/E_0)$, is a stochastic variable. The wave gain is the time integral of the wave energy density growth rate and it is related to the wave elctric field, $E(t)$, by $E^2(t) = E_0^2 \exp[G(t)]$ where E_0 is a constant field. The observed electric field, E, is a consequence of a large number of amplifications and damping:

$$E = E_0 \prod_{i=1}^{N} e^{G_i}, \quad N \gg 1, \tag{2}$$

where G_i (gain) is a stochastic variable. Taking the logarithm of this equation one obtains:

$$\log E = \log E_0 + \sum_{i=1}^{N} G_i. \tag{3}$$

The central limit theorem can then be applied to the probability distribution of $\log E$ which is thus a normal distribution (e.g. Robinson, 1993).

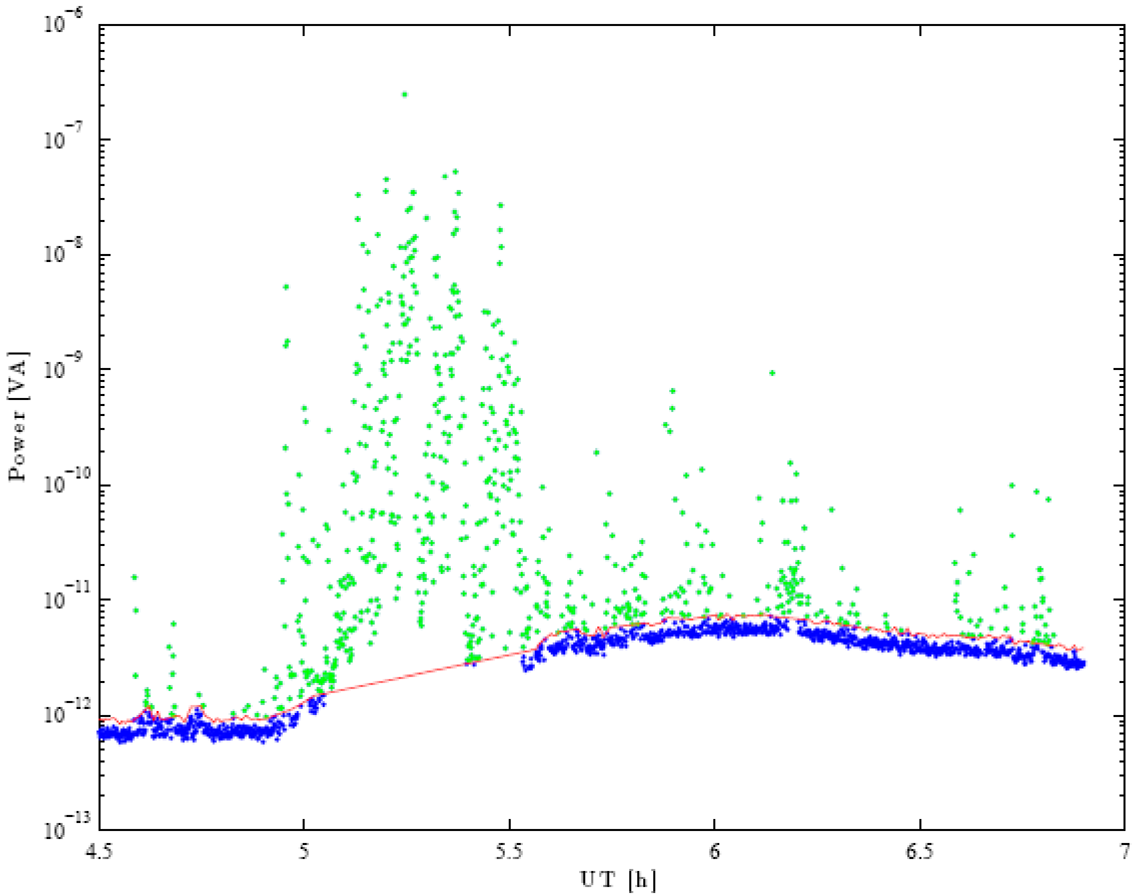

Figure 3. The power of Langmuir waves obtained by integration of the power spectral density over the frequency interval from 8 to 18 kHz around the plasma frequency $f_p = 12$ kHz (2002 October 21st event). The red line separates the power of Langmuir waves (green points) from the background (blue points).

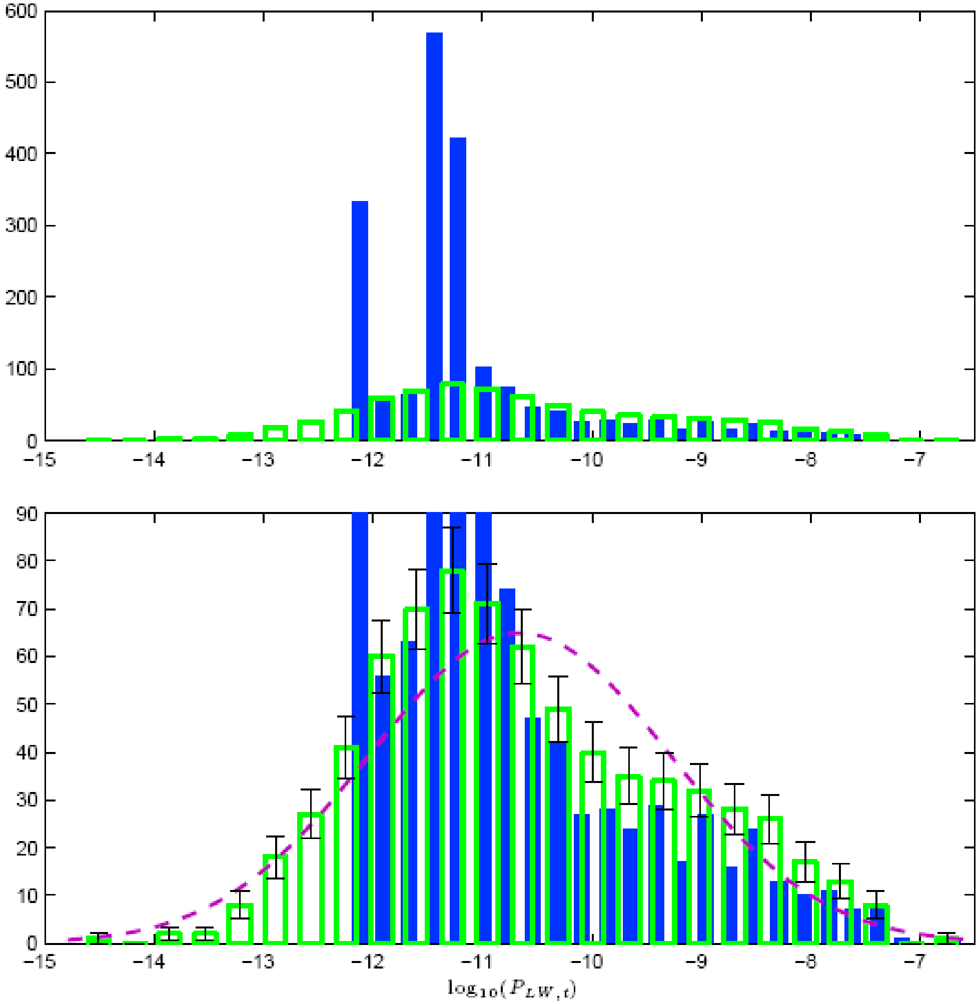

Figure 4. Histograms of Langmuir waves power (2002 October 21st event). Upper panel: Before (blue bars) and after (green bars) background removing. Lower panel: part of upper panel, dashed line represents Gaussian fit of LW power histogram after background removing.

$$\frac{p'(x)}{p(x)} = \frac{b_0 + b_1 x}{c_0 + c_1 x + c_2 x}$$

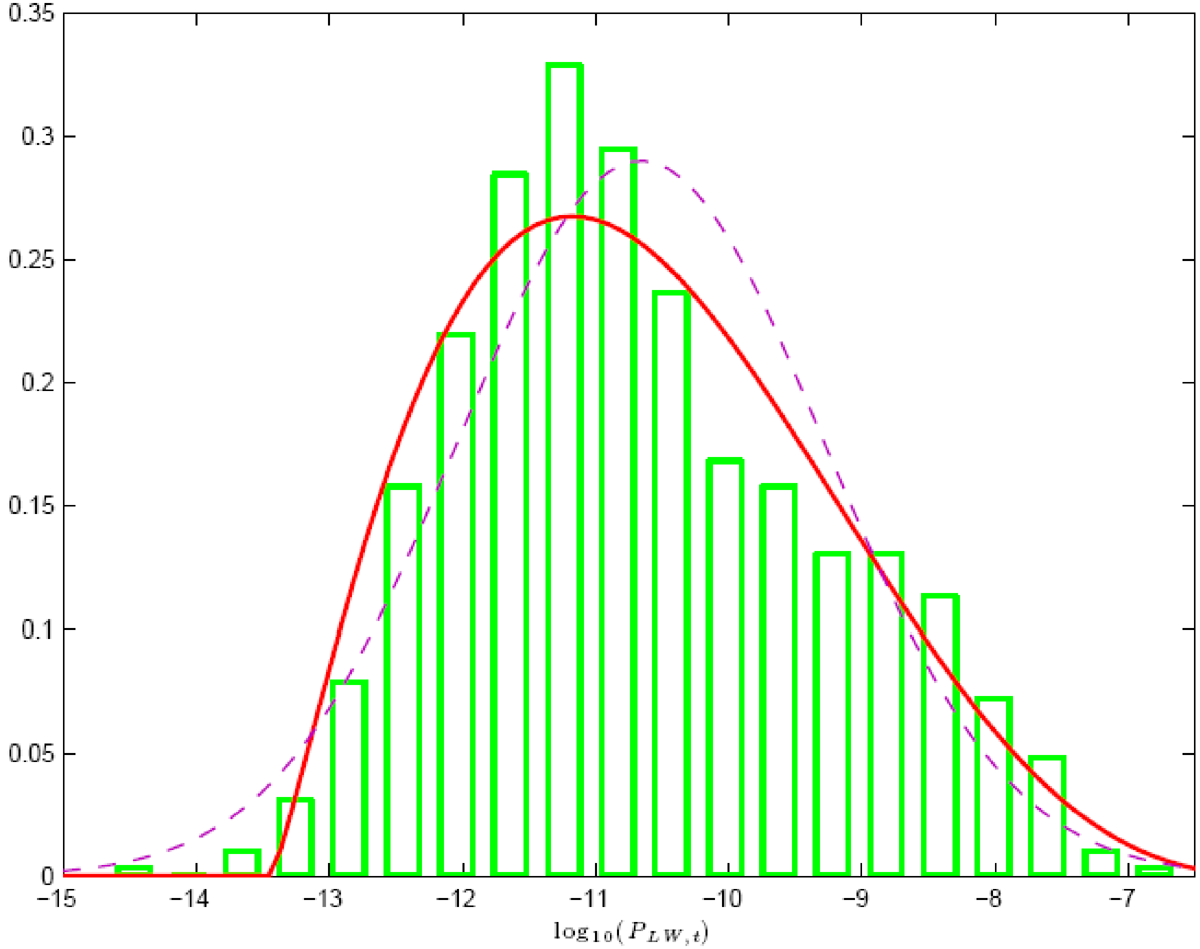

Figure 5. Pearson type I (solid red line) and normal (dashed line) probability density distribution of Langmuir waves power (2002 October 21st event).

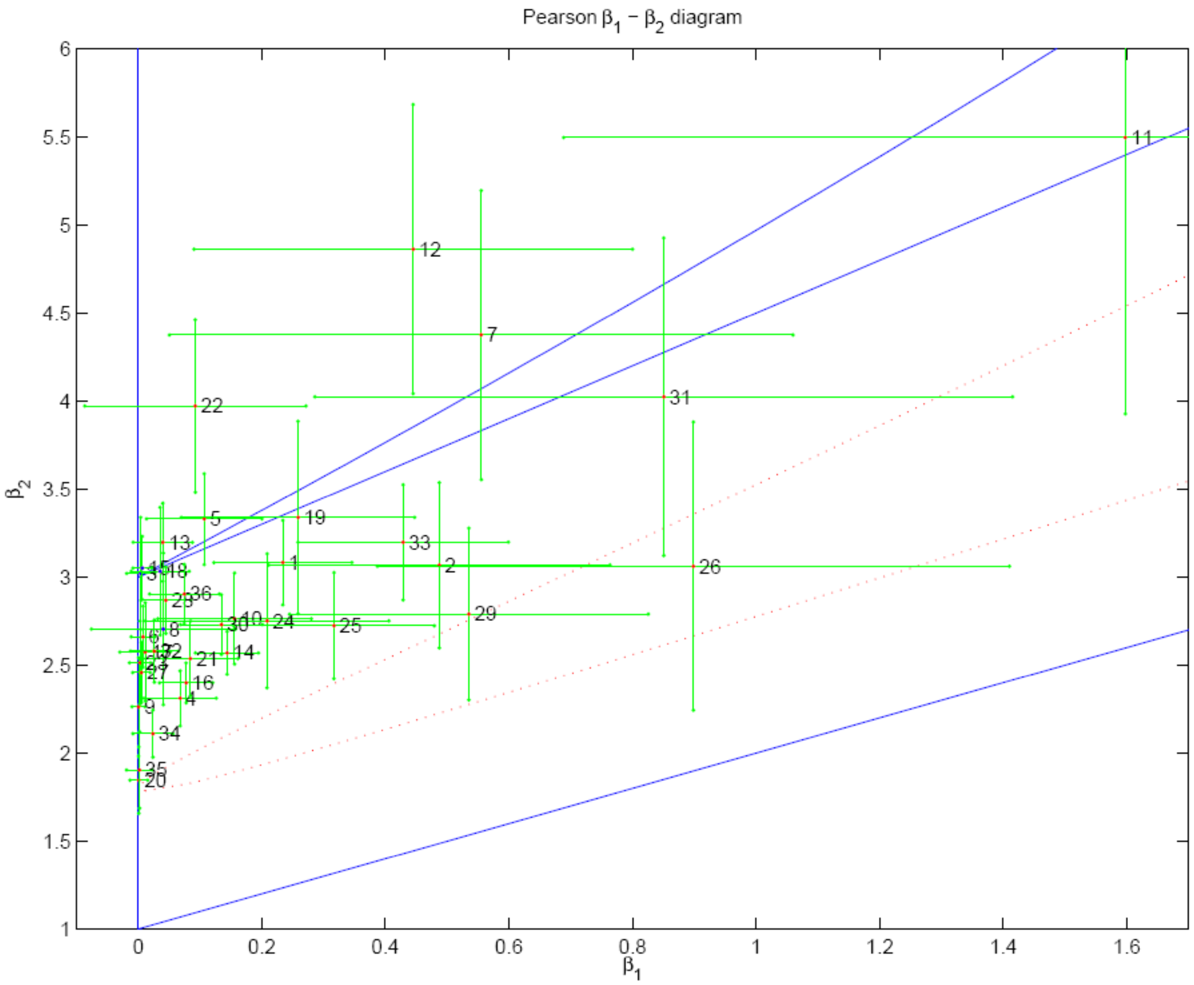

Out of 36 event, 32 have no intersection with Log Normal distribution
(0,3 in the plane)

Open Questions & perspectives

- Emission at Fp, 2Fp, both ?
- Slight linear polarization at high Freq. which disappears at a few MHz. Why ?
- Why a maximum of radio flux energy at 1 MHz (around 6 Rs) ?

Puissance radio rayonnée

$$P(t,f) = \frac{S(t,f,\varphi)\Delta f d^2}{D(f,\varphi)}\Omega$$

Angle solide : $\Omega = \int\int_{4\pi} D(\theta,\phi)d\Omega.$

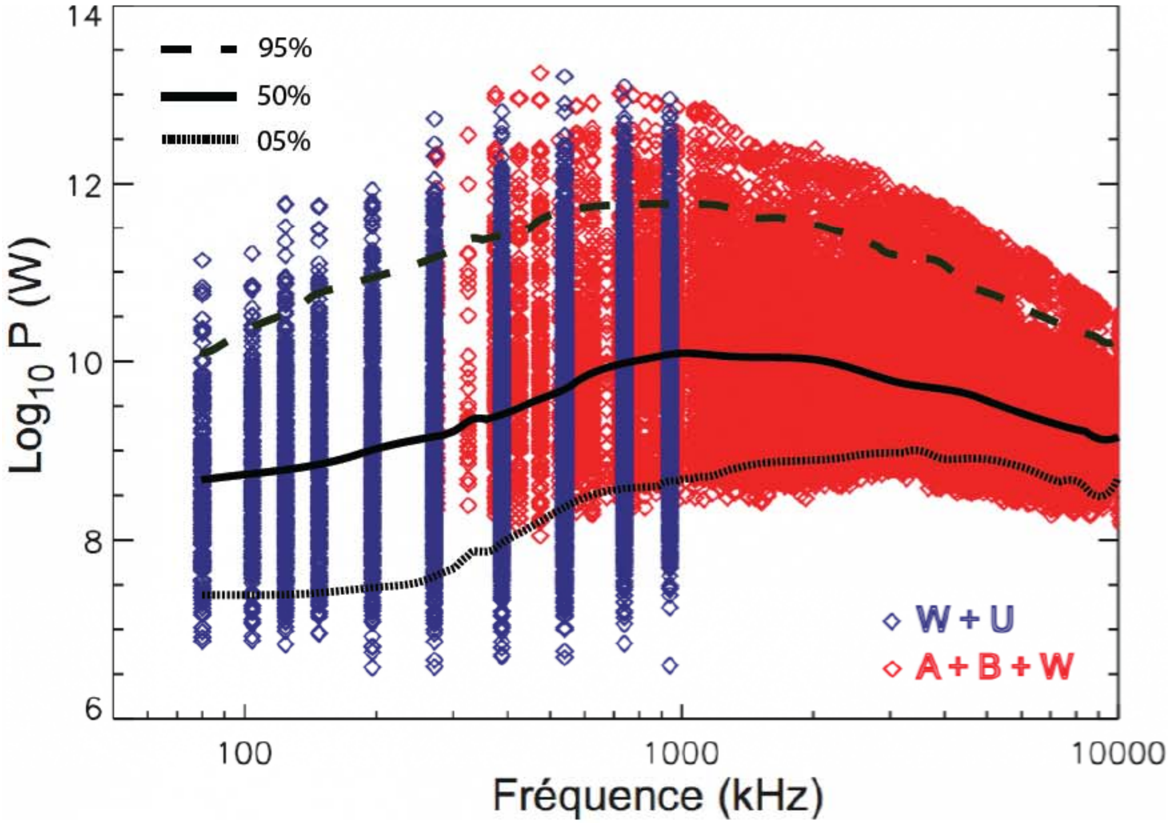

- Distribution de puissance log-normale?
- Maximum autour de ~1 MHz (R ~ 6R$_\odot$)
  - Convergence des faisceaux

    (Dulk et al. 2001)
  - Décélération des électrons + directivité

    (Weber 1978)

Open Questions & perspectives

- ❑ Emission at Fp, 2Fp, both ?
- ❑ Slight linear polarization at high Freq. which disappears at a few MHz. Why ?
- ❑ Why a maximum of radio flux energy at 1 MHz (around 6 Rs) ?
- ❑ Why is the beam decelerated after 1 Mhz (around 6 Rs) ?

Correction par rapport à la radiale

$$v = \frac{1}{\cos(\psi)} \frac{dr}{df} \frac{df}{dt}$$

Dérive en fréquence (données radio)

Profil radial de densité

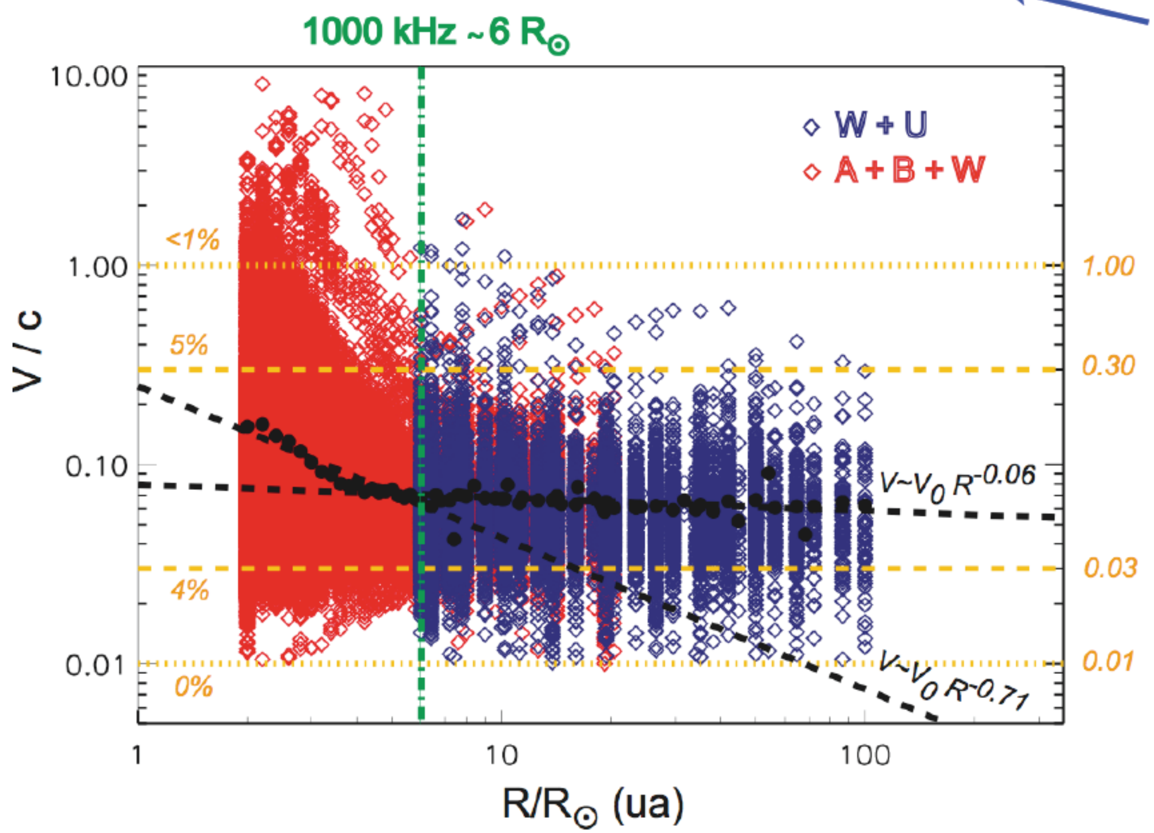

- R < 6 R⊙
  ➡ Décélération “rapide” des électrons du faisceau.
- R > 6 R⊙
  ➡ Décélération “lente” des électrons du faisceau.

$V_{initiale}$ et V_{finale} sont décorrélées.

(Poquérusse et al 1996)

Perte d’énergie cinétique du faisceau plus efficace dans la couronne.
Rôle prédominant des propriétés du milieu ambiant sur les mécanismes d’émission

Open Questions & perspectives

- **Emission at Fp, 2Fp, both ?**
- **Slight linear polarization at high Freq. which disappears at a few MHz. Why ?**
- **Why a maximum of radio flux energy at 1 MHz (around 6 Rs) ?**
- **Why is the beam decelerated after 1 Mhz (around 6 Rs)**
- **The radio flux energy varies by about 6 orders of magnitude. Is it only related to the beam properties ? Is $S_{radio} \propto N_{beam} x E_{beam}^4$ a correct statement ?**
- **Can we infer information on the primary radio beam from the scattered one ?**

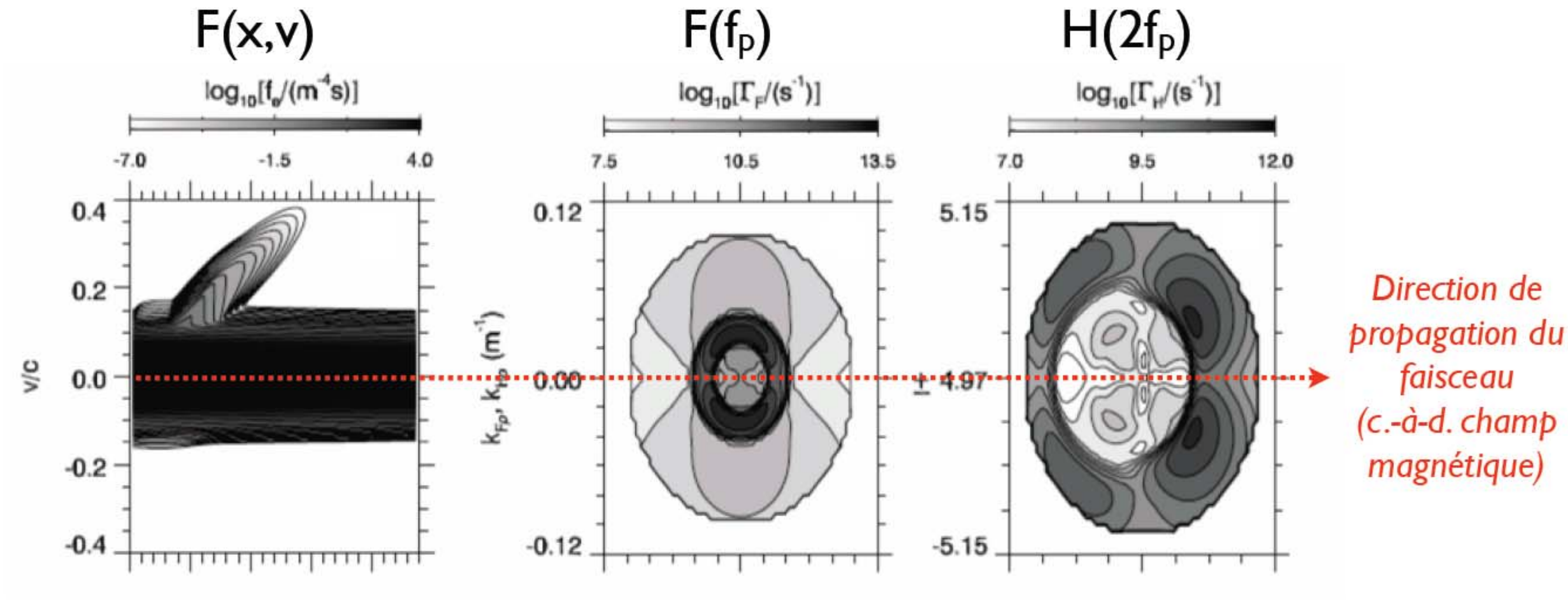

Li et al. 2008

Emission dipolaire

Emission quadripolaire

Diagramme d'émission apparent

Indice de réfraction dans
un plasma (non-magnétisé) → $\mu(f) = \sqrt{1 - \left(\frac{f_p}{f}\right)^2}$

Réfraction du rayonnement
(gradient de densité)

\+

Diffusion du rayonnement
(fluctuations de densité)

$F(f = 1.05 f_p)$

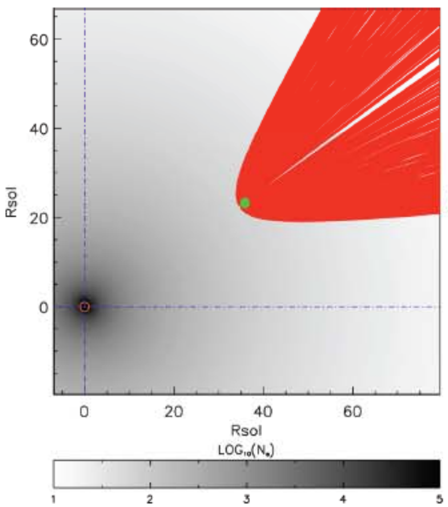

$H(f=2f_p)$

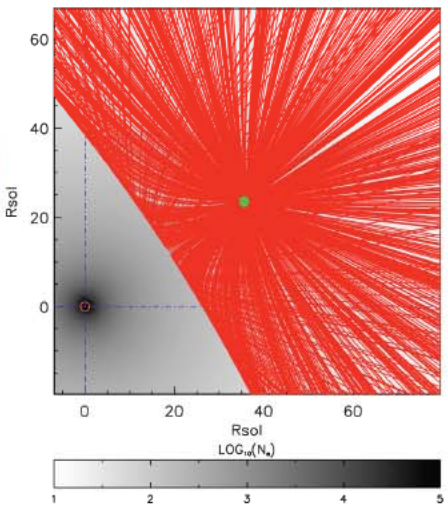

$F(f = 1.05 f_p)$

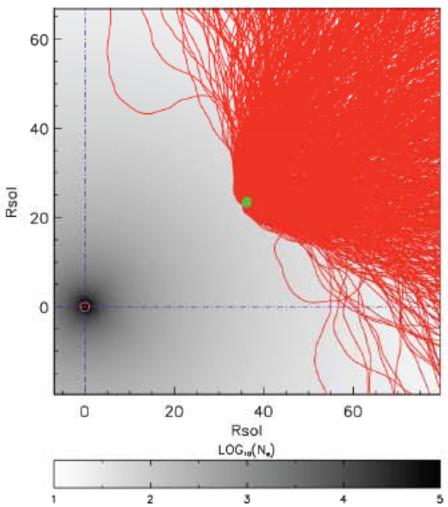

$H(f=2f_p)$

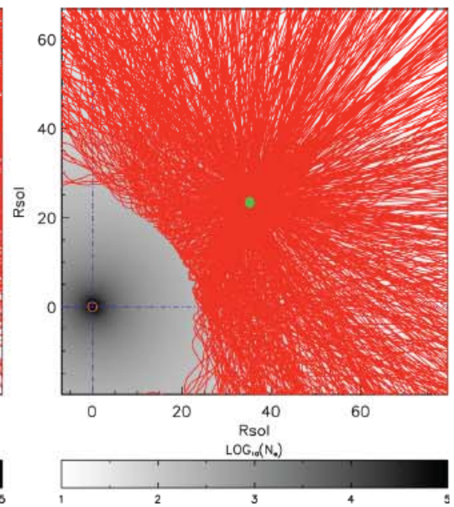

Les effets de propagations modifient le diagramme primaire

Open Questions & perspectives

- ❑ **Emission at Fp, 2Fp, both ?**
- ❑ **Slight linear polarization at high Freq. which disappears at a few MHz. Why ?**
- ❑ **Why a maximum of radio flux energy at 1 MHz (around 6 Rs) ?**
- ❑ **Why is the beam decelerated after 1 Mhz (around 6 Rs)**
- ❑ **The radio flux energy varies by about 6 orders of magnitude. Is it only related to the beam properties ? Is $S_{radio} \propto N_{beam} x E_{beam}^4$ a correct statement ?**
- ❑ **Can we infer information on the primary radio beam from the scattered one ?**
- ❑ **Can we infer properties on the radial evolution of the density fluctuations from the Type III radio scattering ?**
- ❑ **Can we infer properties on the background thermal plasma in the corona from the type III radio emission ? From the X-ray observation**

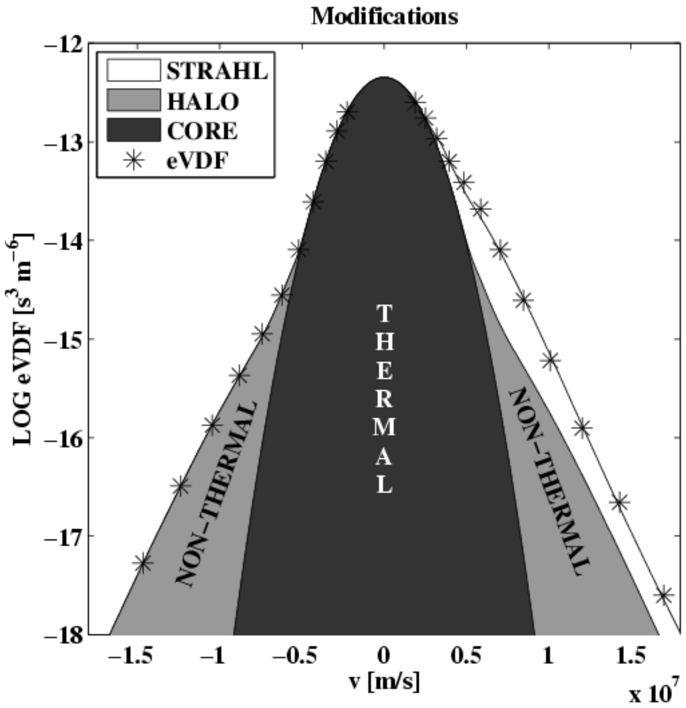

Non-thermal tails in the electron distribution functions could drive the wind :

- **Ambipolar electric field**
- **Enhanced heat flux**

Core : bi-Maxwellian * flat-top

Halo : bi- Kappa * (1-flat-top) from antisunward dir.

Strahl : bi- Kappa * (1-flat-top) from antisunward dir.

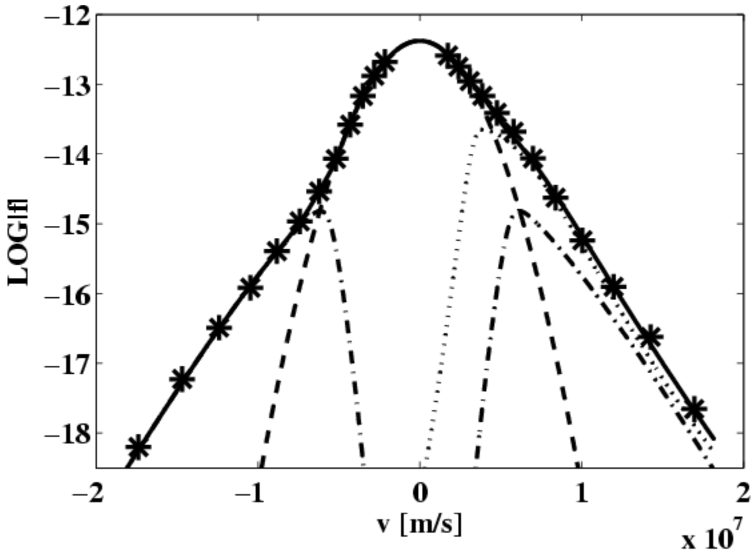

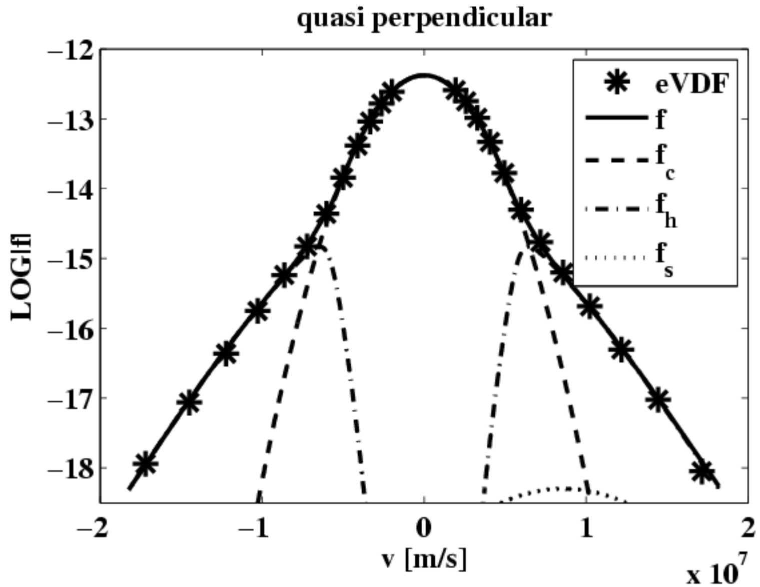

Stverak et al., 2010

- *Interplanetary electric potential*

$$\frac{m_e M G}{r_o} << kT$$

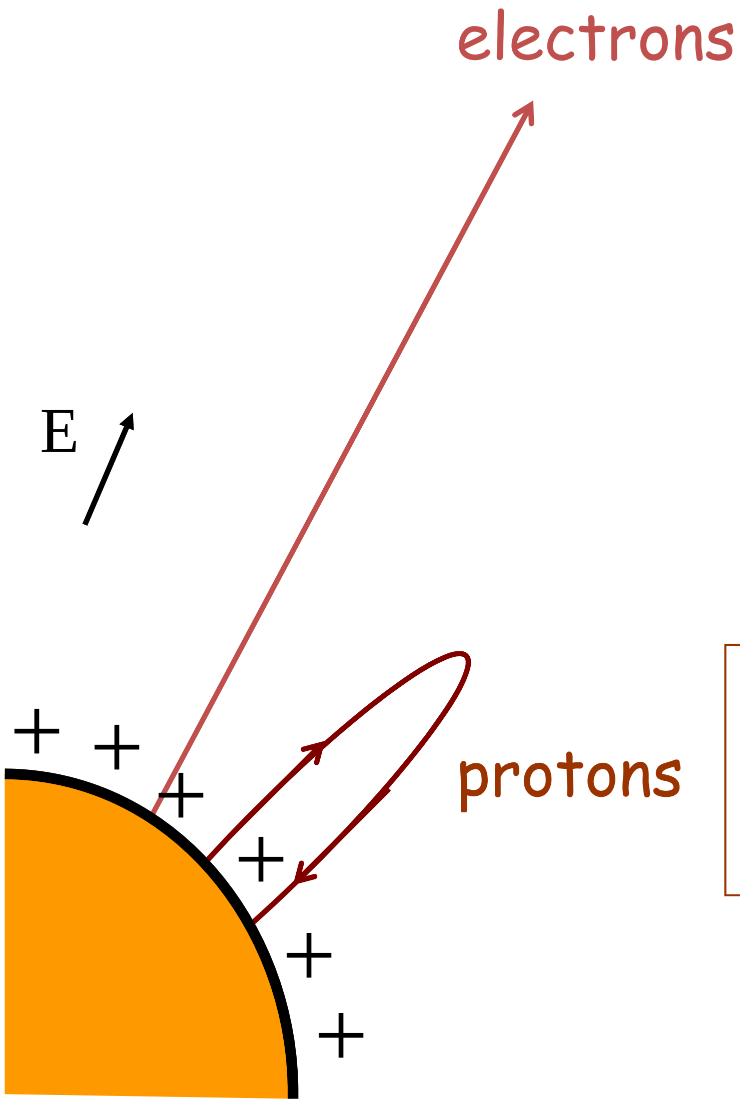

$$\frac{m_p M G}{r_o} > kT$$

- *Interplanetary electric potential*

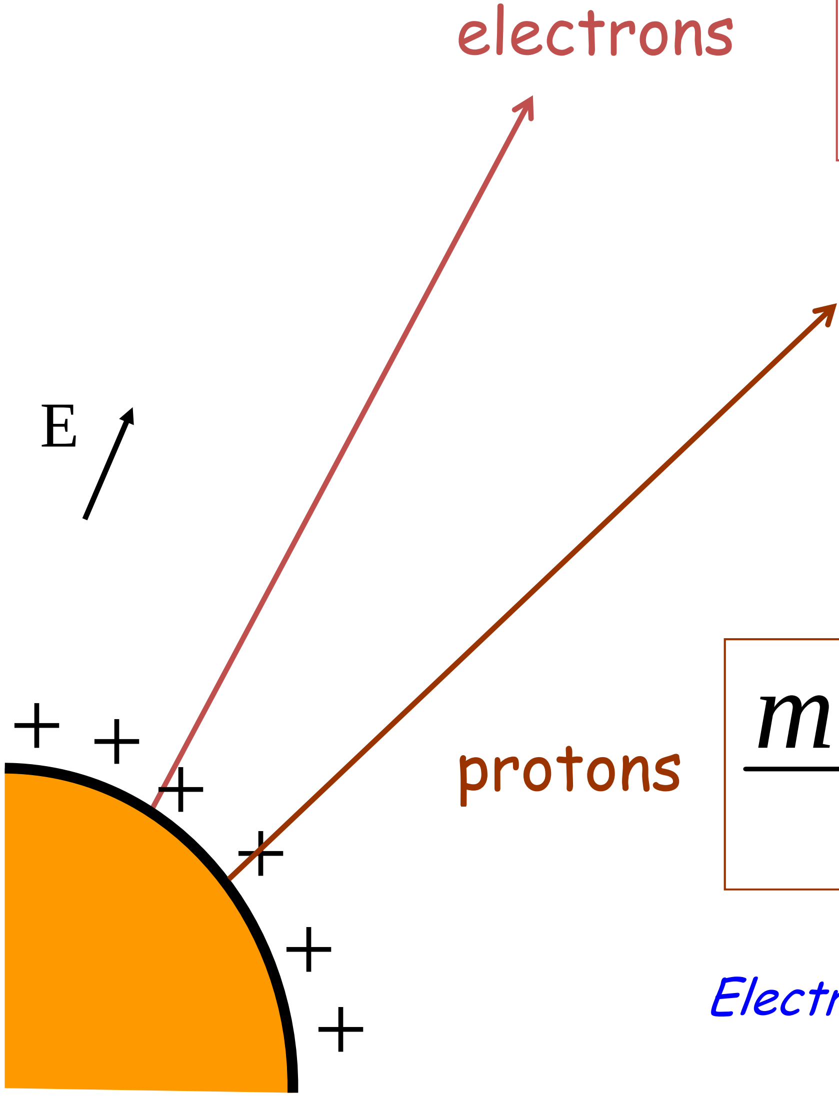

$$\frac{m_e MG}{r_o} << kT$$

$$\frac{m_p MG}{r_o} > kT$$

Electrons are pulling the wind

Helios, Cluster, Ulysses

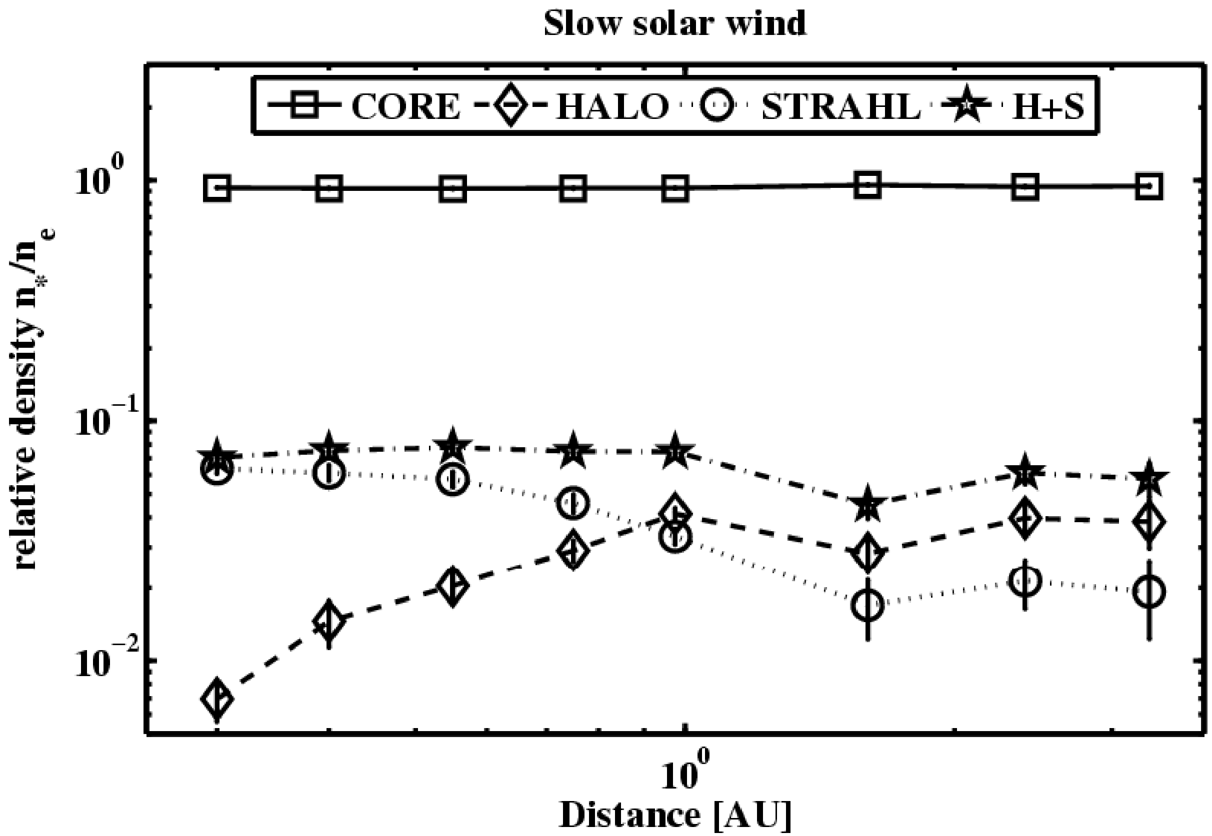

Strahl is transformed into halo with distance
by particle/wave interactions

Similar to fast wind (Maksimovic et al. 2005)

Open Questions & perspectives

- **Emission at Fp, 2Fp, both ?**
- **Slight linear polarization at high Freq. which disappears at a few MHz. Why ?**
- **Why a maximum of radio flux energy at 1 MHz (around 6 Rs) ?**
- **Why is the beam decelerated after 1 Mhz (around 6 Rs)**
- **The radio flux energy varies by about 6 orders of magnitude. Is it only related to the beam properties ? Is $S_{radio} \propto N_{beam} x E_{beam}^4$ a correct statement ?**
- **Can we infer information on the primary radio beam from the scattered one ?**
- **Can we infer properties on the radial evolution of the density fluctuations from the Type III radio scattering ?**
- **Can we infer properties on the background thermal plasma in the corona from the type III radio emission ? From the X-ray observations**
- **How are the langmuir waves converted into e-m emission ?**
- **Why is there a delay between Langmuir waves and beam particles ?**
- **Role of the density fluctuations ?**

Langmuir wave eigenmodes in (preexisting) density structure

Resonant wavelengths are quantized – this has implications for growth, damping, and radiation (see Malaspina talk)

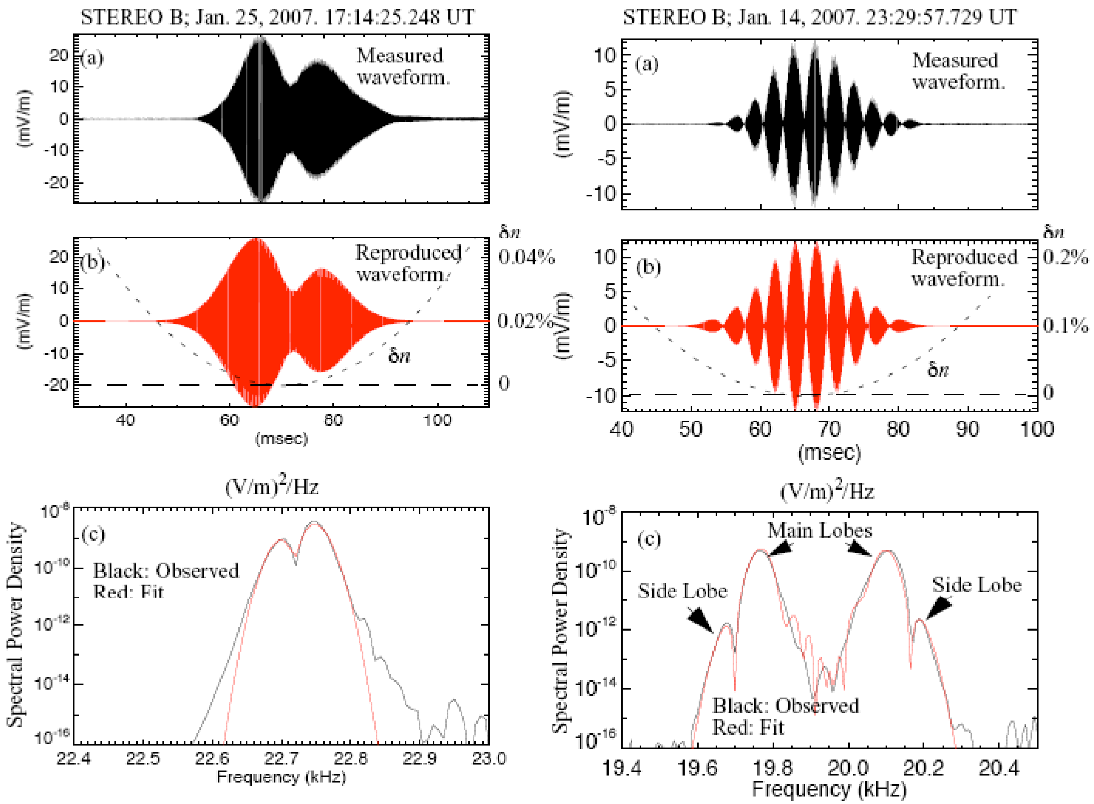

(Ergun et al., 2008)

Open Questions & perspectives

- **Emission at Fp, 2Fp, both ?**
- **Slight linear polarization at high Freq. which disappears at a few MHz. Why ?**
- **Why a maximum of radio flux energy at 1 MHz (around 6 Rs) ?**
- **Why is the beam decelerated after 1 Mhz (around 6 Rs)**
- **The radio flux energy varies by about 6 orders of magnitude. Is it only related to the beam properties ? Is $S_{radio} \propto N_{beam} x E_{beam}^4$ a correct statement ?**
- **Can we infer information on the primary radio beam from the scattered one ?**
- **Can we infer properties on the radial evolution of the density fluctuations from the Type III radio scattering ?**
- **Can we infer properties on the background thermal plasma in the corona from the type III radio emission ? From the X-ray observations**
- **How are the langmuir waves converted into e-m emission ?**
- **Why is there a delay between Langmuir waves and beam particles ?**
- **Role of the density fluctuations ?**
- **Link between ground based radio / X-ray / kilometric range**

Solar Orbiter

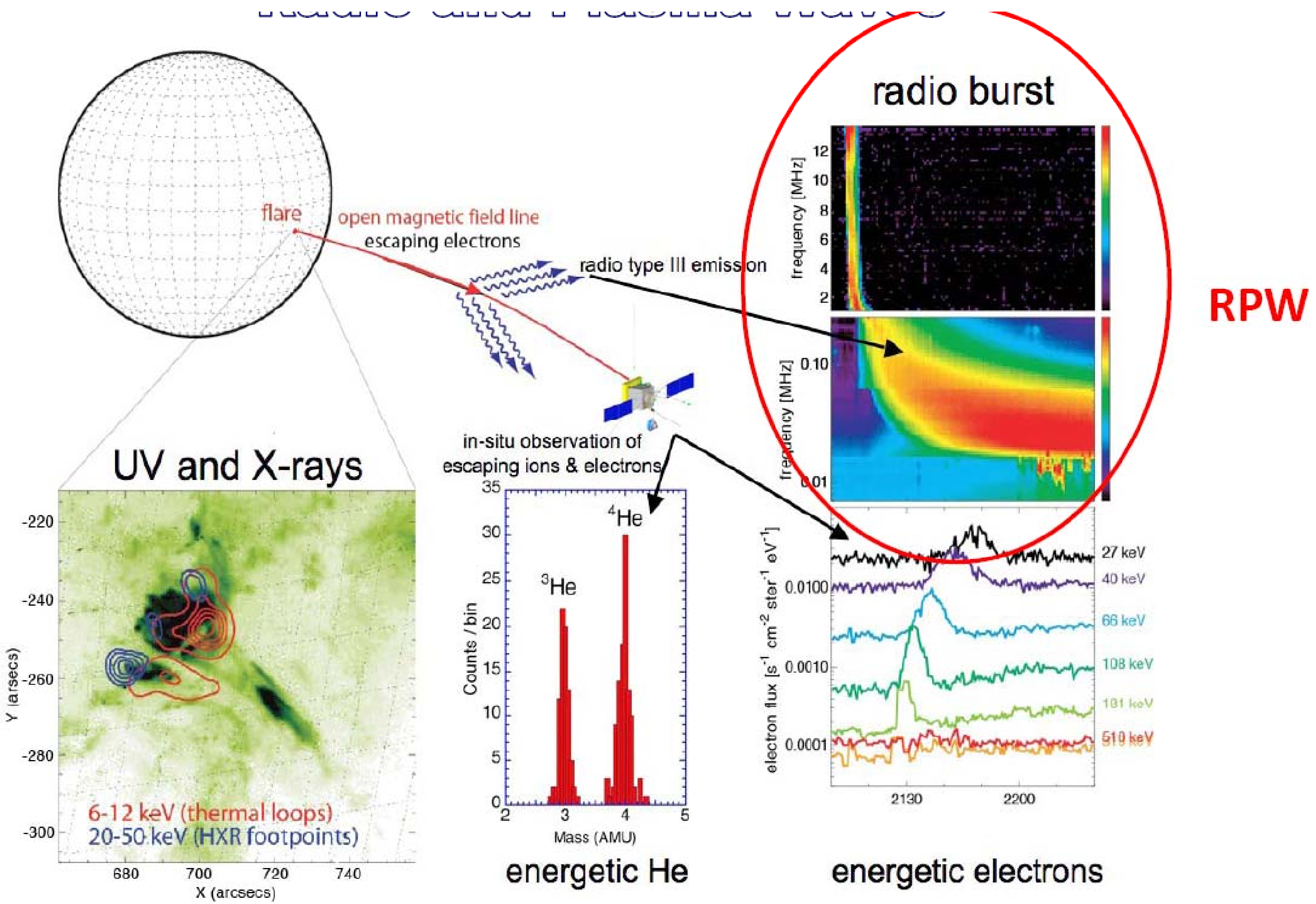

Open Questions & perspectives

- ❑ Emission at Fp, 2Fp, both ?
- ❑ Slight linear polarization at high Freq. which disappears at a few MHz. Why ?
- ❑ Why a maximum of radio flux energy at 1 MHz (around 6 Rs) ?
- ❑ Why is the beam decelerated after 1 Mhz (around 6 Rs)
- ❑ The radio flux energy varies by about 6 orders of magnitude. Is it only related to the beam properties ? Is $S_{radio} \propto N_{beam} x E_{beam}^4$ a correct statement ?
- ❑ Can we infer information on the primary radio beam from the scattered one ?
- ❑ Can we infer properties on the radial evolution of the density fluctuations from the Type III radio scattering ?
- ❑ Can we infer properties on the background thermal plasma in the corona from the type III radio emission ? From the X-ray observations
- ❑ How are the langmuir waves converted into e-m emission ?
- ❑ Why is there a delay between Langmuir waves and beam particles ?
- ❑ Role of the density fluctuations ?
- ❑ Link between ground based radio / X-ray / kilometric range
- ❑ ….

The exospheric approach

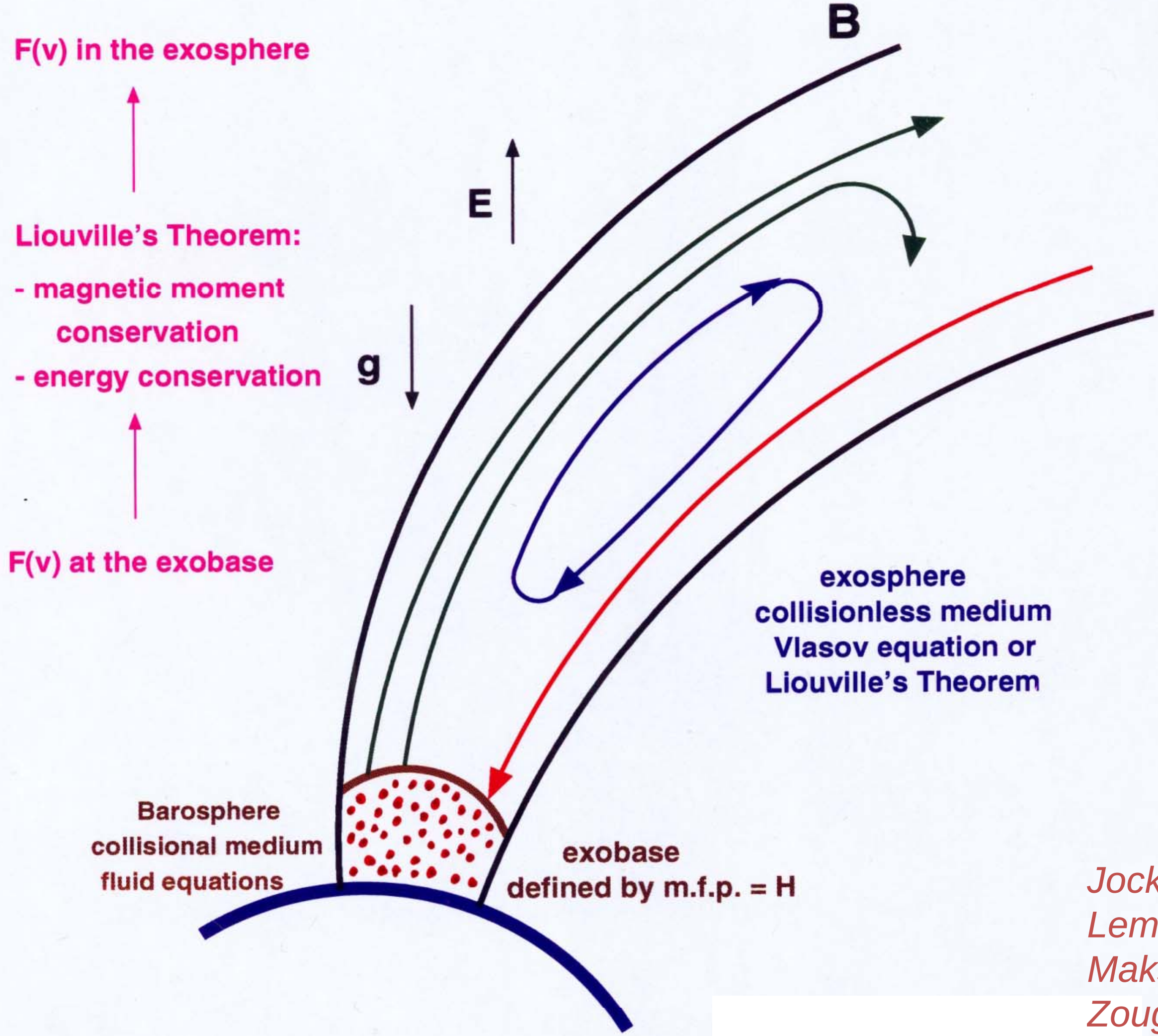

Jockers, 1971
Lemaire & Scherer, 1971
Maksimovic et al., 1997
Zouganelis et al., 2004

Interprétation de la déviation

Déviation du maximum d'émission par rapport à la direction du champ magnétique local

⬇

Existence d'un gradient de densité au voisinage de la source radio
(Poquérusse et al. 1996, Hoang et al. 1997)